Applicability of the DMSO (Dimethyl Sulfoxide) Aggregate Degradation Test to Determine Moisture Induced Distress in Asphalt Concrete Mixes

by

John J. Heinicke
Graduate Research Assistant
Department of Civil Engineering
Oregon State University

Ted S. Vinson
Professor
Department of Civil Engineering
Oregon State University

James E. Wilson
Assistant Engineer of Materials
Oregon Department of Transportation

June 1987

Prepared for
Oregon Department of Transportation
Salem, OR 97310

Technical Report Documentation Page

1. Report No.	2. Government Accession No.	3. Recipient's Catalog No.
FHWA-OR-RD-87		

4. Title and Subtitle

The Use of the IRM_r and DMSO Accelerated Weathering Test to Determine the Potential for Moisture-Induced Distress in Asphalt Concrete Mixtures

5. Report Date
June 1987

6. Performing Organization Code

8. Performing Organization Report No.
TRR: 87-26

7. Author(s)
John J. Heinicke, Ted S. Vinson, and James E. Wilson

9. Performing Organization Name and Address
Transportation Research Institute
Oregon State University
201 Apperson Hall
Corvallis, OR 97331-2302

10. Work Unit No. (TRAIS)

11. Contract or Grant No.
HP&R 085-5167

12. Sponsoring Agency Name and Address
Oregon Dept of Transportation
Highway Division
Materials & Research Section
Salem, OR 97310

US Dept of Transportation
Federal Highway Admin.
Office of Research & Devel.
Washington, DC 20590

13. Type of Report and Period Covered
Final Report
June 1986 - June 1987

14. Sponsoring Agency Code

15. Supplementary Notes

16. Abstract

ODOT employs the dimethyl sulfoxide accelerated weathering test (DMSO test) to identify the potential for degradation of aggregates under high-moisture environmental conditions. A laboratory investigation was conducted to evaluate the effectiveness of the DMSO test to predict moisture-induced distress in asphalt concrete mixtures. Asphalt concrete specimens were fabricated using aggregates from three quarries. The specimens were conditioned using vacuum saturation and a series of five freeze/thaw cycles. The resilient modulus (M_r) was obtained before and after each conditioning cycle and the Index of Retained resilient modulus (IRM_r) was determined. The results indicate the DMSO test may be used to identify the potential for moisture-induced distress in asphalt concrete mixtures. However, no correlation was determined between the DMSO test results and the IRM_r or fatigue life test results.

The strain and temperature dependencies of the M_r were determined for a dense-graded asphalt concrete mixture. It was concluded that constant stress testing may result in a misinterpretation of the IRM_r, and further, tests conducted within the currently accepted temperature range may result in a ±20% deviation in the IRM_r. In an accompanying analytical program, the effect of diametral test boundary conditions on the measured value of M_r was evaluated using two- and three-dimensional finite element models. The results indicate that the resilient modulus diametral test is adequately represented by elastic theory and an assumed plane stress condition.

17. Key Words	18. Distribution Statement
DMSO, accelerated weathering test, moisture-induced distress, stripping, resilient modulus	No restrictions. This document is available to the public through National Technical Information Service (NTIS), Springfield, VA 22161

19. Security Classif. (of this report)	20. Security Classif. (of this page)	21. No. of Pages	22. Price
Unclassified	Unclassified		

Form DOT F 1700.7 (8-72) Reproduction of completed page authorized

TABLE OF CONTENTS

		Page
1.	INTRODUCTION	1
	Problem Statement	1
	Purpose and Scope	1
2.	BACKGROUND	3
	Moisture-Induced Distress of Asphalt Concrete Mixtures	3
	Aggregate Properties that Affect Adhesion	4
	The DMSO Test	7
	Tests to Indicate Moisture Susceptibility of Asphalt Concrete Mixtures	8
3.	TESTS MATERIALS AND PROCEDURE	16
	Aggregate Sources	16
	Mix Design	19
	The Resilient Modulus Test	21
	Fatigue Life Test	22
	Test Procedure	22
4.	RESULTS AND DISCUSSION	25
	Resilient Modulus Tests	25
	Fatigue Life Tests	30
	Comparison of Test Results and Aggregate Durability	37
5.	CONCLUSIONS	42
6.	RECOMMENDATIONS-IMPLEMENTATION	44
7.	REFERENCES	45
8.	APPENDICES	
	A- Influence of Boundary Conditions on the Determination of Resilient Modulus	48
	The Resilient Modulus Test	48
	Finite Element Representation of the Test Condition	56

TABLE OF CONTENTS

	Page
B- Strain and Temperature Dependency of the IRMr	66
Laboratory Test Program	66
Test Results	67
Discussion of Results	69
C- Asphalt Properties and Mix Design Data	76
D- Asphalt Properties and Mix Design Data	78
E- Resilient Modulus and Fatigue Life Test Data	86

ACKNOWLEDGEMENT

This report presents the results from a Highway Planning and Research study conducted by the Oregon State Highway Division of the Oregon Department of Transportation (ODOT) and Oregon State University in cooperation with the Federal Highway Administration.

The contribution of Glenn Boyle and the staff of the Bituminous Mix Design Group of the ODOT Materials Section in obtaining materials and preparing test specimens was invaluable and greatly appreciated.

DISCLAIMER

LIST OF FIGURES

Figure		Page
1	Reduction of the Contact Angle Between Asphalt Cement and Aggregate in the Presence of Water (after Tyler, 1938)	5
2	Nomalized Dynamic Modulus vs. Shear Strain (after Seed and Idriss, 1970)	14
3	Quarry Locations of Aggregate Sources Used to Fabricate Asphalt Concrete Specimens	17
4	Flow Chart of Test Program	23
5	Resilient Modulus and Index of Retained Resilient Modulus vs. Conditioning Cycle	26
6	Effects of Asphalt Aging on Control Specimens	29
7	Corrected Index of Retained Resilient Modulus vs. Conditioning Cycle	29
8	Fatigue Life vs. Initial Tensile Strain	31
9	Fatigue Life vs. Tensile Stress	32
10	Comparison of Fatigue Life Curves	34
11	Percent Increase of Initial Tensile Strain vs. Percent Fatigue Life	36
12	Predicted Shift in Fatigue Life Curves Associated with Increase of the Initial Tensile Strain	38
13	Percent Change of Resilient Modulus vs. Percent Fatigue Life	39
A.1	Test Specimen with Diametral Yoke and Loading Ram	49
A.2	Definition Sketch of a Diametrally Loaded Circular Element	51
A.3	Unit Stress Distribution Along the Vertical and Horizontal Axes for a Diametrally Loaded 4-inch Diameter Circular Element with a 0.5-inch Strip Load (after Hondros, 1959)	52
A.4	Meshes Utilized in Finite Element Analyses	58
A.5	Comparison of Unit Stress Distributions	64
B.1	Resilient Moduli vs. Tensile Strain for the Temperature Range of 36°F to 92°F	68
B.2	Normalized Resilient Moduli vs. Tensile Strain	72
B.3	Envelope and Average Relationship for Normalized Resilient Moduli vs. Tensile Strain	73
B.4	Resilient Modulus vs. Temperature at a Tensile Strain of 100 μ	73

LIST OF TABLES

Table		Page
1	Petrographic Analyses of Selected Aggregate Sources	18
2	Summary of Durability Tests for Selected Aggregate Sources	18
3	Summary of Mix Design	20
4	Regression Constants for Fatigue Life Test Relationships	33
A.1	Results of Finite Element Analyses	61
B.1	Regression Constants for Log Tensile Strain vs. Log Resilient Modulus Relationships	70

NOTATION

a	=	width of loading strip
E	=	elastic modulus
H	=	total recoverable horizontal deflection
H(int)	=	horizontal deflection of interior node of finite element model
H_l	=	horizontal deflection over the length l in the center of the test specimen
IRM_r	=	index of retained resilient modulus
l	=	length in the center of the specimen over which the strain is measured
Mr	=	resilient modulus
n, K	=	regression coefficients
P	=	repeated load
r	=	radial distance from the origin of the test specimen
R	=	radius of the test specimen
R^2	=	coefficient of correlation
t	=	thickness of test specimen
TSR	=	tensile strength ratio
V	=	total recoverable vertical deflection
2α	=	angle at origin subtended by the width of the loading section
ε_t	=	tensile strain in the center of the specimen

NOTATION

υ = Poisson's ratio

μ = microstrain

σ_{rx} = tangential stress along the horizontal axis

$\sigma_{\theta x}$ = radial stress along the horizontal axis

σ_{ry} = tangential stress along the vertical axis

$\sigma_{\theta y}$ = radial stress along the vertical axis

σ_{rx}^{*} = tangential unit stress along the horizontal axis

$\sigma_{\theta x}^{*}$ = radial unit stress along the horizontal axis

σ_{ry}^{*} = tangential unit stress along the vertical axis

$\sigma_{\theta y}^{*}$ = radial unit stress along the vertical axis

1.0 INTRODUCTION

Problem Statement

The Oregon Department of Transportation (ODOT) has long recognized that quality aggregate resources are becoming scarce in many parts of the state. Consequently, various aggregate degradation tests have been employed in an attempt to ensure that quality aggregates are used in roadway structures. Some basaltic rocks common to the State of Oregon exhibit excellent mechanical durability, but degrade and disintegrate when exposed to moisture and/or freeze-thaw cycles. For this reason, the dimethyl sulfoxide accelerated weathering test (DMSO test) has been developed to predict degradation under high-moisture environmental conditions.

Szymoniak et.al. (1986) established the applicable limits of the DMSO weight loss parameter for base course (unbound) aggregates. At present, the applicability of the DMSO test is not known for aggregates that are subsequently employed in asphalt concrete pavements. Specifically, there is no existing correlation between the DMSO weight loss and the moisture susceptibility of an asphalt concrete mixture.

Purpose and Scope

The purpose of this study is to establish the applicability of the DMSO test to determine the potential for moisture-induced distress in asphalt concrete mixtures. The scope of work was limited to laboratory tests performed on asphalt concrete mixtures prepared using crushed rock from three quarries in the State of Oregon: 1) Baker Rock, 2) Meacham, and 3) Ochoco Mile-Post 60. Specimens measuring 4-inches in diameter by 2.5-inches in height were fabricated using standard ODOT procedures (Sullivan et.al., 1986). The specimens were subjected to the Lottman

conditioning procedure (Lottman, 1978), which was modified to include five freeze/thaw cycles. Resilient modulus tests were performed after each cycle to evaluate the reduction of modulus (i.e. index of retained resilient modulus, IRM_r). Fatigue life tests were performed following the last freeze/thaw cycle. Finally, the results from these mechanical tests were compared to the DMSO weight loss for the aggregates.

2.0 BACKGROUND

Moisture-Induced Distress of Asphalt Concrete Mixtures

Many asphalt pavements in Oregon deteriorate before reaching their intended design life. Much of this premature damage results from the pavement's exposure to moisture, a problem that is accelerated in areas subjected to repeated freeze-thaw cycling (Hicks et.al., 1985). Currently, ODOT is spending $500,000/year for lime treatment of aggregates in an attempt to improve the moisture resistance of the aggregate employed in asphalt concrete pavements (Frederickson, 1987). Approximately 100 million dollars are budgeted yearly for pavement maintenance in the State of Oregon, but the amount specifically used to repair moisture-induced damage is unknown (Sullivan, 1987).

Asphalt concrete mixtures provide strength, or stiffness, through cohesive resistance of the asphalt cement binder and aggregate interlock and frictional resistance between aggregate particles. A mixture's stiffness is fully mobilized when the adhesive bond between the binder and the aggregate is completely developed. For this case, any failure plane through the material must initiate in the binder. However, when moisture penetrates the pavement, it may emulsify within the binder and/or weaken the adhesive bond. Thus, the presence of moisture results in a loss of stiffness.

Moisture-induced distress may be associated with: 1) the loss of mix cohesion, or physical changes of the asphalt cement binder, 2) the loss of adhesion between the asphalt cement and the aggregate, or stripping, and 3) the degradation of the aggregate from the effects of water. Although these phenomena may occur simultaneously, the visual

evidence of moisture-induced distress (i.e. flushing, ravelling, and random cracking and potholing) is related to stripping. Indeed, past and current literature concerning moisture related pavement damage pertains almost exclusively to stripping. Thus, stripping is generally implied in any discussion of moisture-induced distress. With this perspective, the remaining discussion addresses the problem of stripping.

Stripping involves the weakening of the adhesive bond between the asphalt cement and the aggregate. The strength of the bond depends upon complex physio-chemical forces and interactions between the asphalt cement, the aggregate, water, and air. There are three commonly accepted theories of adhesion, and five proposed mechanisms to explain the occurrence of the stripping phenomenon (Majidzadeh and Brovold, 1968; Taylor and Khosla, 1983; Fromm, 1974).

In simple terms, stripping can be viewed as the reduction of the contact angle between the asphalt cement and the aggregate. Water enters the pavement structure and is preferentially attracted to the aggregate, and physically separates the aggregate from the binder. This concept is illustrated in Figure1.

Aggregate Properties that Affect Adhesion

Although aggregates constitute from 90% to 95% of the weight of an asphalt concrete mixture, their effect on the moisture susceptibility of the mixture is not necessarily proportional to the relative ratio of the amount of aggregate to the amount of asphalt cement (Rice, 1958). Rather, the quality of the adhesive bond between the aggregate and the asphalt cement is responsible for the mixture's behavior upon exposure to water. This interfacial bond involves the surface areas of both the binder

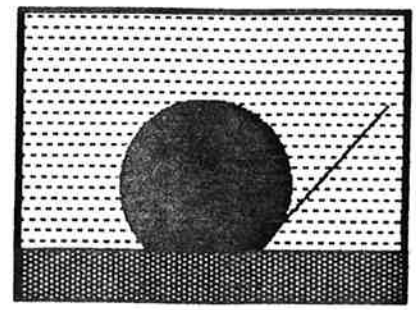

(1) When the aggregate with a drop of asphalt cement contacts water, the contact angle is less than 90°.

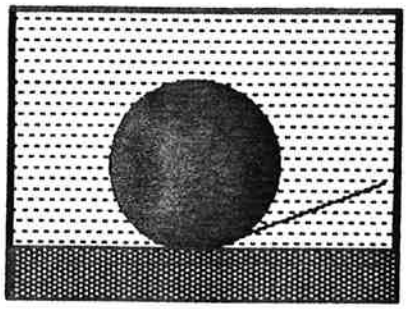

(2) As the water begins to remove the asphalt cement, the contact angle is reduced.

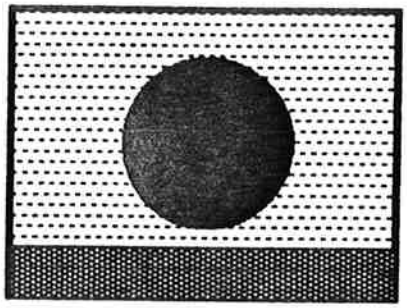

(3) Finally, the contact angle is 0°, and the asphalt cement has stripped.

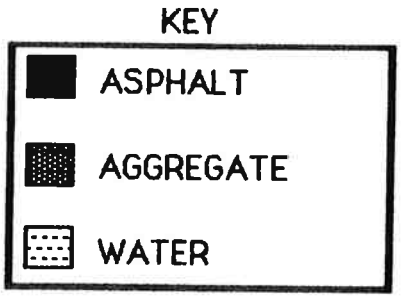

FIGURE 1. Reduction of the Contact Angle Between Asphalt Cement and Aggregate in the Presence of Water (after Tyler, 1938).

and the aggregate. Obviously, the surface areas of the aggregate and the asphalt cement are equal at the bond interface. Thus, the degree of adhesion achieved at this bond depends upon the asphalt cement properties, the aggregate properties, and the conditions under which the bond is formed (Majidzadeh and Brovold, 1968). A discussion of the asphalt cement properties and the conditions of formation is beyond the scope of this paper. A brief review of important aggregate properties follows.

The mineralogical composition of the aggregate is the most important factor that influences adhesion (Majidzadeh and Brovold, 1968; Rice, 1958). The presence of unbalanced surface charges and adsorbed coatings has a direct influence on the strength of any bond that forms on the aggregate's surface. The nature of the surface forces determines the chemical reactions that can occur, and thus controls the mixture's behavior in the presence of water. Aggregates are generally divided into two groups: 1) hydrophobic and 2) hydrophilic. Further, it is commonly believed that basic aggregates are hydrophobic and that acidic aggregates are hydrophilic. Although this is a good generality, some investigators have found it to be incorrect (Karius and Dalton, 1964; Schmidt and Graf, 1972).

Particle size is another important factor that influences adhension , especially with regard to the fine portion of aggregate in the mixture. The finer sizes have a larger surface area exposed, and the surface charges of these sizes have an effect much greater than their proportion by weight in the mixture. Further, since the fines may coat the aggregate surface, the bond formed at the interface may be more dependent upon the surface

energies of the fines rather than the coarse aggregate. The presence of fines also increases the viscosity of the binder, thus reducing the coatability. However, if an adequate initial coating is achieved, the resistance to stripping is also increased owing to the higher viscosity (Ishai and Craus, 1977).

Other aggregate properties that influence adhesion include the surface texture and porosity. Surface texture affects the coatability and mechanical retention of asphalt cement to the aggregate. Porosity increases the mechanical interlock between the asphalt cement and the aggregate, but may detrimentally affect the mixture if water is retained in the pores prior to mixing. In addition, the particle shape and gradation may have some effect upon the adhesive bond.

The DMSO Test

The DMSO weight loss parameter is an index value that is used to predict the behavior of unbound aggregate in the presence of water. Aggregates with a high DMSO weight loss are identified as unsuitable for use as base course material. However, it is not known if such aggregate could be successfully bound by asphalt cement.

DMSO is a penetrant that enters the rock matrix and reacts with deleterious materials (smectite clays). The interaction of DMSO with clay minerals involves two processes: 1) DMSO penetrates the rock and solvates cations held on mineral surfaces, and 2) DMSO dehydrates large anions by donating hydrogen ions. Thus, the DMSO test reflects the mineralogy of the rock and, further, may to some degree predict the amount of deleterious fines produced during the crushing process. Since the mineralogical composition and the fines content of the aggregate are

the major factors affecting the strength of the adhesive bond between the aggregate and the binder, it is reasonable to assume that the DMSO test may indicate potential stripping problems. Therefore, the attempt to relate the DMSO index with indices used to evaluate stripping is justified.

Tests To Indicate Moisture Susceptibility of Asphalt Concrete Mixtures

Traditionally, tests designed to indicate the moisture susceptibility of asphalt concrete mixtures have been performed on either loose or compacted specimens. Tests utilizing compacted specimens are preferred for several reasons : 1) a test on a laboratory compacted specimen generally provides the investigator with a mechanical property of the paving material, 2) field cores, cut to standard dimensions, can be tested for mechanical properties with the paving mix at the field condition to correlate the laboratory results to the field, and 3) the interpretation of many of the tests which utilize loose specimens is subjective; therefore the results of such tests may be biased by the preconceived ideas of the investigator.

In 1978, Lottman presented a procedure for the accelerated conditioning of laboratory compacted test specimens (Lottman, 1978). This procedure consists of preparing nine 4-inch diameter by 2.5-inch thick specimens, which are divided into three sets (three specimens per set). Three specimens remain in a dry condition, three are subjected to vacuum saturation, and three are subjected to vacuum saturation followed by one freeze-thaw cycle. Lottman utilized the indirect tensile splitting test, with a constant loading rate to failure, to measure the tensile strength of each specimen. The results of these tests are combined to obtain the tensile strength ratio (TSR). Following an extensive five year

field study, it was concluded that if the TSR > 0.80, the mixture will provide an adequate level of service with respect to moisture-induced distress (Lottman, 1982).

Lottman's investigation clearly indicates that two distinct test phases must be employed in the determination of moisture-induced distress: 1) the test specimen must be subjected to a laboratory conditioning procedure (e.g. the Lottman procedure), and 2) a mechanical property of the material, that reflects the degree of induced damage, must be measured. Although some investigators question the severity of the Lottman procedure (Tunnicliff and Root, 1984), many pavement engineers agree that it provides a reasonable assessment of conditions under which moisture damage may occur in the field.

Three groups have recently identified the use of an index of retained resilient modulus (IRM_r) to assess the moisture susceptibility of asphalt concrete mixes (Hicks et.al., 1985; Graf,1986; Stuart, 1986). The IRM_r is determined from the following relationship:

$$IRM_r = \frac{M_r \text{ of conditioned specimen}}{M_r \text{ of dry (control) specimen}} \qquad (2.1)$$

These investigators provide independent corroboration of the use of the IRM_r as a predictor of moisture-induced distress. The study by Hicks et.al (1985) is particularly significant as it represents the first use of the IRM_r to predict the moisture susceptibility of asphalt concrete mixtures with known field performances. Based on their work, the criteria

for the IRM_r were established as follows:

$IRM_r > 0.70$ ==> mix passes as designed

$IRM_r < 0.70$ ==> mix fails and must be redesigned

The resilient modulus is a material property that is directly related to the load carrying capacity, or stiffness, of a flexible pavement. The IRM_r represents the ratio of two moduli, and is based on the premise that the disturbance to an asphalt concrete mixture associated with moisture-induced distress will cause a subsequent reduction in the modulus value of an undisturbed mixture. Thus, the IRM_r may be viewed as an index property that represents the reduction of stiffness caused by a given level of disturbance. Obviously, the IRM_r of moisture susceptible mixtures should have a value less than one.

Two distinct test phases are required to evaluate the IRM_r: 1) the test specimen must be conditioned in some manner to simulate environmental conditions in the field, and 2) the resilient modulus must be evaluated. Test specimens utilized in the determination of the IRM_r are generally subjected to the Lottman conditioning procedure (Hicks et.al., 1985; Graf,1986; Stuart, 1986). The Lottman procedure, which involves vacuum saturation followed by a freeze/thaw cycle, has been criticized as being too severe (Tunnicliff and Root, 1984). However, Lottman has provided photographic evidence displaying similar types of material damage in both laboratory conditioned specimens and field cores and, further, successfully correlated laboratory specimens to the deterioration of asphalt pavements (Lottman, 1978 and 1982).

It may be noted that specimen conditioning is a procedural matter

rather than a problem inherent in the test method (Taylor and Khosla, 1983). Indeed, the conditioning procedure could be modified to simulate local climatic conditions. Kelly et.al. (1986) determined that repeated freeze/thaw cycling was necessary to differentiate between the benefits of various antistripping additives, and to identify the stripping potential of some aggregates. In their investigation, the Lottman procedure was modified to include five freeze/thaw cycles, and the IRM_r was determined following each conditioning cycle.

The use of the IRM_r is based upon the premise that disturbance associated with moisture-induced distress in an asphalt concrete mixture will cause a reduction in the modulus value when compared to the same mixture in an unconditioned or undisturbed state. This concept is justified from a material science standpoint and from the work of others outside the realm of pavement engineering. For example, geotechnical engineers have long recognized that disturbance resulting from soil sampling techniques can cause reductions in the modulus values of soils returned to the laboratory. As a result, correction factors as large as 2 to 5 are applied to laboratory determined moduli to represent in situ conditions (Lambe and Whitman, 1969; Bjjerum, 1964; Seed and Idriss, 1970). If these correction factors are considered as ratios of the disturbed modulus divided by the undisturbed modulus, values of 0.5 to 0.2 result. In an analagous manner, the IRM_r may be viewed as an index property that represents the reduction of stiffness in an asphalt concrete mix resulting from a given level of disturbance. The advantages of using the resilient modulus test to assess moisture-induced distress in asphalt concrete

mixes include:

1) The resilient modulus is directly affected by the loss of adhesion and cohesion.
2) The resilient modulus test mobilizes small strains in the specimen. Under small strains, the material approaches the elastic range of its stress-strain response. Further, a low strain level is desirable to avoid damaging the specimen.
3) The resilient modulus test is non-destructive. Fewer specimens are needed to provide the same level of confidence as the TSR, and the effects of continued conditioning cycles can be determined.
4) The test utilizes routinely prepared laboratory specimens.

The major disadvantage of the resilient modulus test is that the equipment is expensive and not available in many facilities. However, as the pavement engineering industry moves from empirical design procedures to the mechanistic design procedure, which is reflected in the new AASHTO design guidelines (1986), resilient modulus testing can be expected to become routine.

The resilient modulus is determined following a standard test procedure (ASTM D 4123), in which a repeated load is applied to a cylindrical specimen along any diametral axis and the displacements are measured along a perpendicular axis (ASTM, 1983). The theory that supports the calculation of a diametrally obtained resilient modulus is based on the assumption of plane stress, and the actual boundary conditions of the test apparatus are ignored. The resulting deviation in the measured value of resilient modulus owing to these assumptions is not

known.

It may be noted from an examination of the standard that the resilient modulus is substantially different under varying test conditions. For example, a modulus obtained at a cold temperature under a load of low duration and high frequency, may be significantly greater than a modulus obtained at a warm temperature under a load of high duration and low frequency. This suggests a need to identify specific test condition parameters (i.e., temperature, load magnitude, load frequency, load duration, and load wave form) to assure that equivalent moduli are being compared in the determination of the IRM_r.

ASTM D 4123 recommends a load range that would induce 10% to 50% of the test specimen's tensile strength. The level of strain mobilized within the specimen during the test is not considered a variable in the standard test procedure. Hicks (1987) suggests that the applied load should generate a strain level between 50 and 150 microstrain units (μ) at the center of the specimen. However, there is presently no specification that requires the same strain level for each modulus test used in the determination of the IRM_r. The significance of the strain level is recognized in the field of geotechnical engineering with respect to the determination of the dynamic modulus for soils under earthquake loading conditions (Seed and Idriss, 1970). The relationship between the shear strain and the normalized dynamic modulus appears in Figure 2. Normalized values of dynamic modulus are utilized so that tests performed using different testing procedures on various soil types can be represented together. If a similar relationship exists between tensile strain and resilient modulus, constant stress level tests to determine

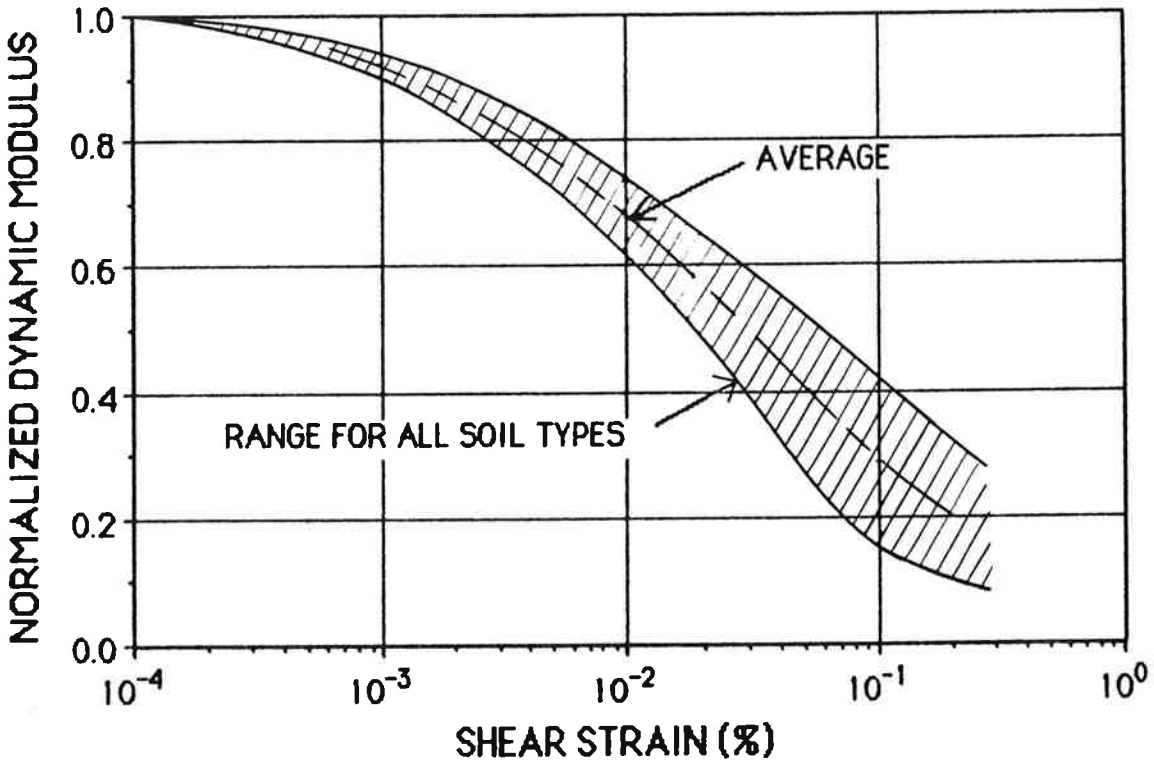

FIGURE 2. Normalized Dynamic Modulus vs. Shear Strain (after Seed and Idriss, 1970).

moduli for use in the IRM_r will result in a misinterpretation of the index property. Material condition parameters of the test specimen can also create variability in IRM_r results. These parameters include: 1) air voids content, 2) degree of saturation, 3) type and number of conditioning cycles, 4) age of the specimen, and 5) compaction method used to fabricate the specimen.

The consequences of slight deviations in the measured value of resilient modulus can be appreciated by considering an example calculation of the IRM_r at a nominal value of 0.70, the threshold value between passing or failing a given mix design. If the moduli of both the dry (control) specimen and the conditioned specimen vary by ±5% from their "true" value, the resulting IRM_r can vary from 0.63 to 0.77. Clearly, slight deviations from a standard test procedure may easily result in a ±5% variation in modulus, and thus influence the decision to either pass or fail a mix design. Therefore, the effects of test condition parameters and material parameters must be recognized to ensure that equivalent or standard moduli are employed in the calculation of the IRM_r. In recognition of this potential problem, two studies were conducted to ascertain 1) the influence of boundary conditions on the determination of resilient modulus, and 2) the strain and temperature dependency of the IRM_r. The results from these studies are presented in Appendices A and B.

3.0 TEST MATERIALS AND PROCEDURE

Aggregate Sources

Of the eight basaltic rock quarries studied by Szymoniak et.al. (1986), three were selected as aggregate sources for the present investigation based upon the following criteria: 1) the availability of a sufficient quantity of the same material tested by Szymoniak et.al. (1986), and 2) the aggregates had to encompass a range of DMSO weight losses. Crushed rock from Baker Rock Quarry (mid-section), Ochoco MP60 Quarry, and Meacham Quarry best satisfied these criteria. The location of these quarries is shown in Figure 3.

Data from the report of Szymoniak et.al. (1986) are in Tables 1 and 2. The results of petrographic analyses appear in Table 1. Table 2 presents the results of both the mechanical durability tests and the DMSO tests. An abbreviated description of each quarry follows.

Baker Rock Quarry is divided into three units with distinct geological characteristics. The mid-section is composed of unfractured, uniformly dense, and very fine-grained rock, which has been oxidized by groundwater in some areas and is unoxidized elsewhere. The mineral contents of Table 1 reflect the differences between these two areas, with the unoxidized area containing a high percentage of smectite clays. The aggregate used in this study represents an equal mixture of each area. The average mineral contents are 68% primary and 29% secondary. Mechanical durability tests and the DMSO weight loss index identify this aggregate as the most undesirable of the three selected sources.

The Ochoco MP-60 Quarry is generally unfractured and composed of fine-grained rock. The mineral contents are 70% primary and 30%

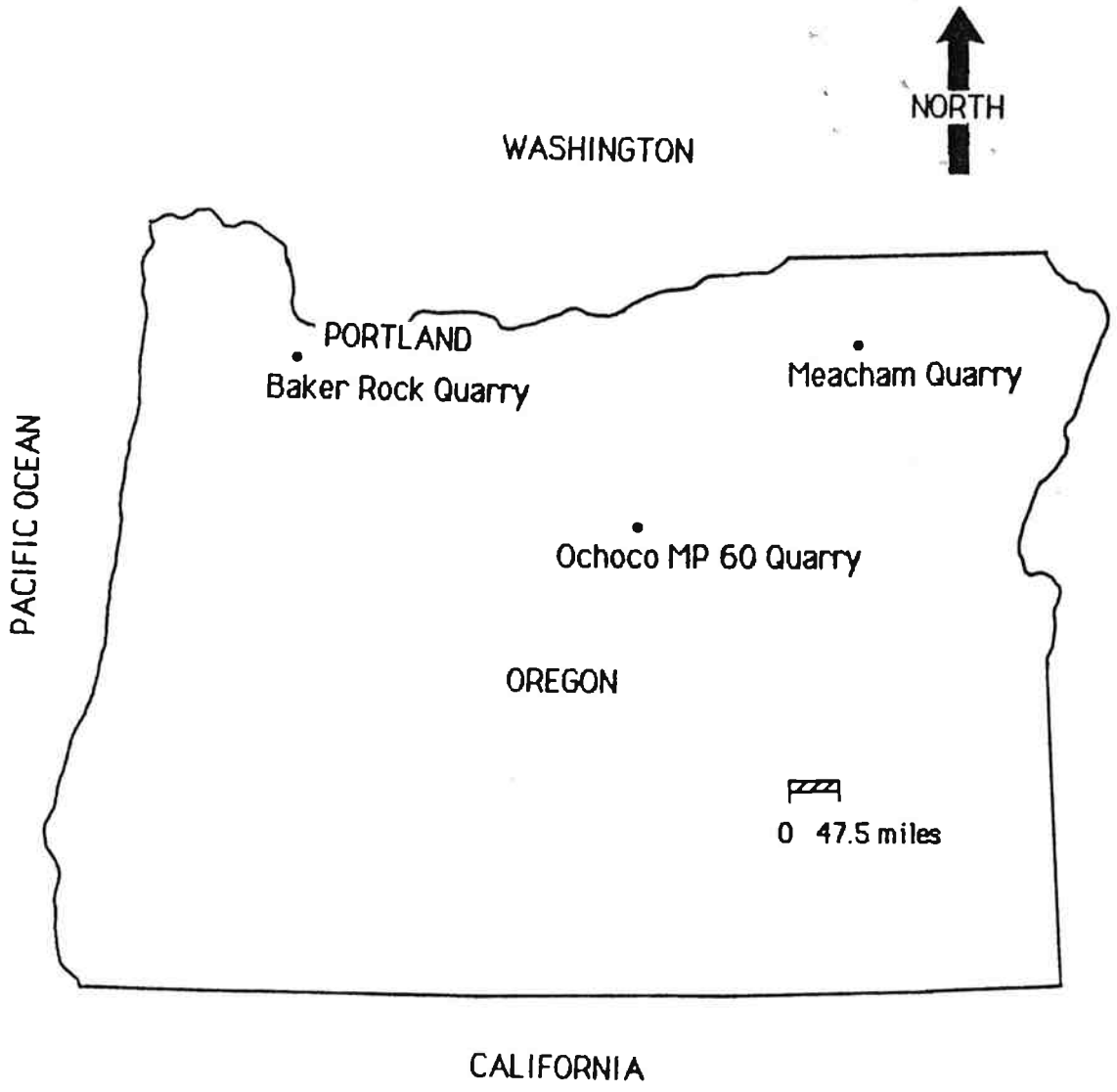

FIGURE 3. Quarry Locations of Aggregate Sources Used to Fabricate Asphalt Concrete Specimens.

TABLE 1. Petrographic Analyses of Selected Aggregate Sources.

QUARRY	PLAGIOCLASE	OLIVINE	PYROXENE	MAGNETITE/ ILLMENITE	SMECTITE CLAY	IRON OXIDE	SEPIOLITE
Baker Rock							
unoxidized	37	5	3	10	31	4	10
oxidized	52	1	19	7	3	18	--
Meacham	36	--	15	11	21	18	--
Ochoco	54	--	9	7	30	--	--

TABLE 2. Summary of Durability Tests for Selected Aggregate Sources.

	SODIUM SULFATE SOUNDNESS % WEIGHT LOSS		OREGON AGGREGATE DEGRADATION		LOS ANGELES ABRASION	DMSO ACCELERATED WEATHERING % WEIGHT LOSS	
QUARRY	COARSE AGGREGATE	FINE AGGREGATE	SEDIMENT HT. (cm)	% PASSING #20 SIEVE	% WEAR	SZYMONIAK 1986	ODOT 1987
Baker Rock	4.8	13.8	2.5	16.6	17.6	17.7	23.9
Meacham	1.7	7.7	--	--	--	8.6	12.6
Ochoco	4.6	9.9	2.8	13.5	16.4	49.3	44.9

secondary, with all secondary minerals being smectite clays. The rock has good mechanical durability properties, but also has a very high DMSO weight loss. Szymoniak (1986) relates the high weight loss to the presence of calcite in the plagioclase matrix. The calcite causes the DMSO to overreact and, thus, it is argued that this material should perform much better than indicated by the DMSO weight loss parameter.

Meacham Quarry rock is highly fractured, dense, and very fine-grained. The rock is comprised of 61% primary minerals and 39% secondary. Although the rock has a high secondary mineral content, it is the most durable according to mechanical durability tests and has the lowest DMSO index. Therefore, this source is expected to display the best mechanical behavior of the three sources.

In qualitative terms, the aggregates were expected to perform as follows with respect to moisture susceptibility:

- Baker Rock Quarry = = > poor
- Ochoco MP 60 Quarry = = > fair to good
- Meaham Quarry = => very good

Mix Design

Four groups of specimens (six specimens per group) were fabricated following standard ODOT procedures (Sullivan et.al., 1986). A summary of the mix designs is given in Table 3. The mix design data and the asphalt properties appear in Appendix D. The only variable originally proposed for this study was the type of aggregate employed in the mix or, specifically, the aggregate's DMSO weight loss parameter. To control the test variables, the same aggregate gradations and asphalt cement were used for all specimens. However, at the inception of the test program, a

TABLE 3. Summary of Mix Designs

AGGREGATE GRADATION	
Size	Combined Dry Sieve %
1"	--
3/4"	100
1/2"	98
3/8"	80
1/4"	62
#10	32
#40	16
#200 (Dry)	4.5

Asphalt Supplier/Grade: Chevron AC-20

GROUP NUMBER	AGGREGATE SOURCE	ASPHALT CONTENT	MAXIMUM SPECIFIC GRAVITY	AVERAGE AIR VOIDS CONTENT
1	Baker with 1% Lime	6.2%	2.480	4.8%
2	Baker	6.2%	2.480	5.5%
3	Meacham	6.2%	2.483	4.4%
4	Ochoco	6.5%	2.364	3.5%

decision was made to design and test mixtures that would be approved for use in the field. Thus, there is some variation other than aggregate type among the groups of specimens. Specifically, there are differences in asphalt cement contents and air voids contents.

The asphalt content of Group 4 was increased to 6.5% to achieve the required value of IRM_r of 0.70. Also, the mix design for the Baker Rock Quarry aggregate required 1.0% lime treatment. Therefore, two groups of specimens (one with lime and one without lime) were prepared using Baker rock. Finally, note that the average air voids contents vary among the four groups of specimens. A small change in air voids content can have a dramatic effect on the IRM_r results, since greater air voids allows more water to enter the specimen.

The Resilient Modulus Test

Resilient modulus test data were obtained following ASTM D 4123. This procedure involves subjecting a cylindrical test specimen to a repeated load along its diametral axis, and measuring the recoverable horizontal deflection on a perpendicular axis. The record of load and deflection are input to the following equations to obtain the resilient modulus and the tensile strain:

$$M_r = .62\ (P/Ht) \qquad (3.1)$$

$$\varepsilon_t = .52\ H \times 10^6 \qquad (3.2)$$

where M_r= resilient modulus (psi)

P = repeated load (lb.)

H= total recoverable horizontal deflection (inch)

t= specimen thickness (inch)

ε_t= tensile strain at the center (microstrain, μ)

Fatigue Life Test

Fatigue life tests involve applying a repeated load to the test specimen until failure by fracture occurs. For this study, fatigue life is defined as the number of load repetitions required to create a 0.25-inch wide vertical crack across the diameter of the specimen. The results of fatigue life tests may be presented as the logarithm of fatigue life versus the logarithm of the initial tensile strain or the initial tensile stress. Fatigue life is then expressed by an equation of the following form:

$$N_f = C\,(1/\varepsilon_{ti})^m \qquad (3.3)$$

or

$$N_f = K\,(1/\sigma_t)^n \qquad (3.4)$$

where N_f= number of load cycles to failure

C, m, K, n = regression constants

ε_{ti}= initial tensile strain (μ)

σ_t= tensile stress (psi)

The initial tensile strain is calculated from Equation 3.2, and the tensile stress at the center of the specimen is calculated as follows:

$$\sigma_t = 0.156\,(P/t) \qquad (3.5)$$

Test Procedure

A flow chart of the test procedure followed in this investigation is shown in Figure 4. Five specimens were randomly selected from each group of six test specimens for conditioning. The IRM_r was established for

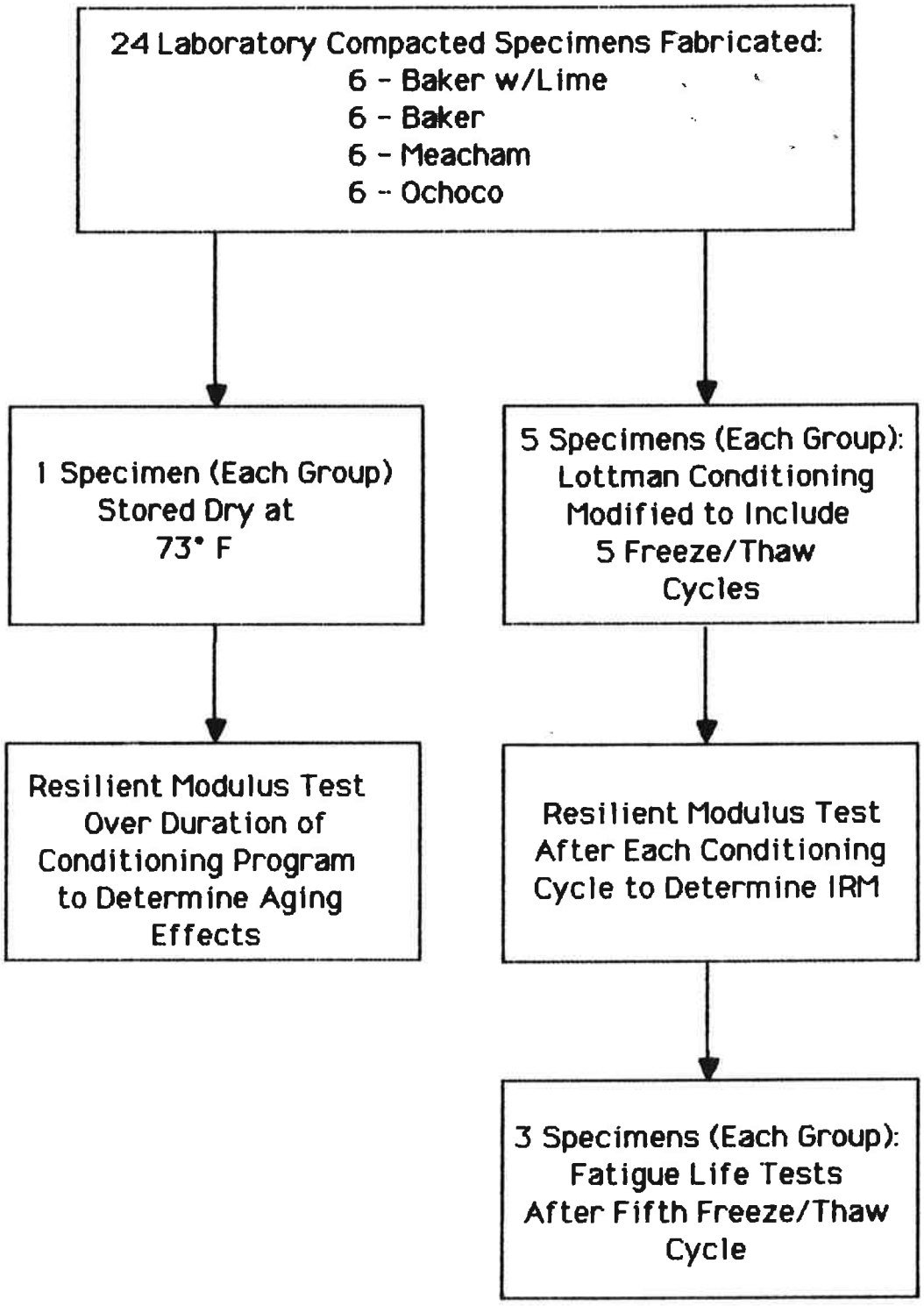

FIGURE 4. Flow Chart of Test Program.

each specimen as follows:

1) determine M_r for the test specimen in dry condition;
2) vacuum saturate the test specimen at 20-inches of Hg for one hour (note: Lottman recommends 26-inches Hg for 1/2 hour);
3) determine M_r for the saturated specimen;
4) freeze the saturated specimen at 0°F for 15 hours;
5) place the frozen specimen in a 140°F water bath for 24 hours;
6) place the specimen in a 73°F water bath for 3 hours; and
7) determine M_r.

Steps 4 through 7 were repeated until each specimen had been subjected to five freeze/thaw cycles. The resilient moduli reported herein were evaluated at 73°F ± 1.8°F using a load frequency of 1 Hz and a load duration of 0.1 second. Further, the moduli were determined at a tensile strain level of 100 μ.

The test specimens were stored in a water bath at 73° F ± 1.8°F after five freeze/thaw cycles, and fatigue life tests were performed over the next 10 days. Three fatigue life tests were performed on each of the four mixtures under investigation. A load of the same duration and frequency used for the resilient modulus tests was applied to induce initial tensile strains of approximately 100μ, 150μ, and 200μ.
One specimen from each group was kept in a dry condition at 73°F. Resilient moduli were determined over the 12 day testing period to quantify the increase of modulus associated with the aging of the asphalt.

4.0 RESULTS AND DISCUSSION

The results reported herein represent 164 resilient modulus tests and 12 fatigue tests performed on four groups of specimens. Tabulated results of all tests are given in Appendix E.

Resilient Modulus Tests

The resilient moduli and IRM_r values for each mixture and conditioning cycle are presented in Figures 5a and 5b, respectively. Each column or data point represents the average of five tests. A review of the data indicates the following:

1) The IRM_r values of the untreated Baker rock mixture decline throughout the conditioning program and indicate that this is the most moisture susceptible mixture.
2) Lime treatment of the Baker aggregate improves the mixture's performance. However, the beneficial effect is not distinguished until the second freeze/thaw cycle. This is consistent with results obtained by Kelly, et.al. (1986).
3) In general, the Meacham and Ochoco rock mixtures have equivalent performances. The Meacham rock mixture has a slightly larger IRM_r after vacuum saturation and the final freeze/thaw cycle. However, the IRM_r values of the Ochoco rock mixture are higher from the first to the fourth freeze/thaw cycle.
4) Although the IRM_r values of the Meacham rock mixture are high, the average values of resilient moduli are lower than the

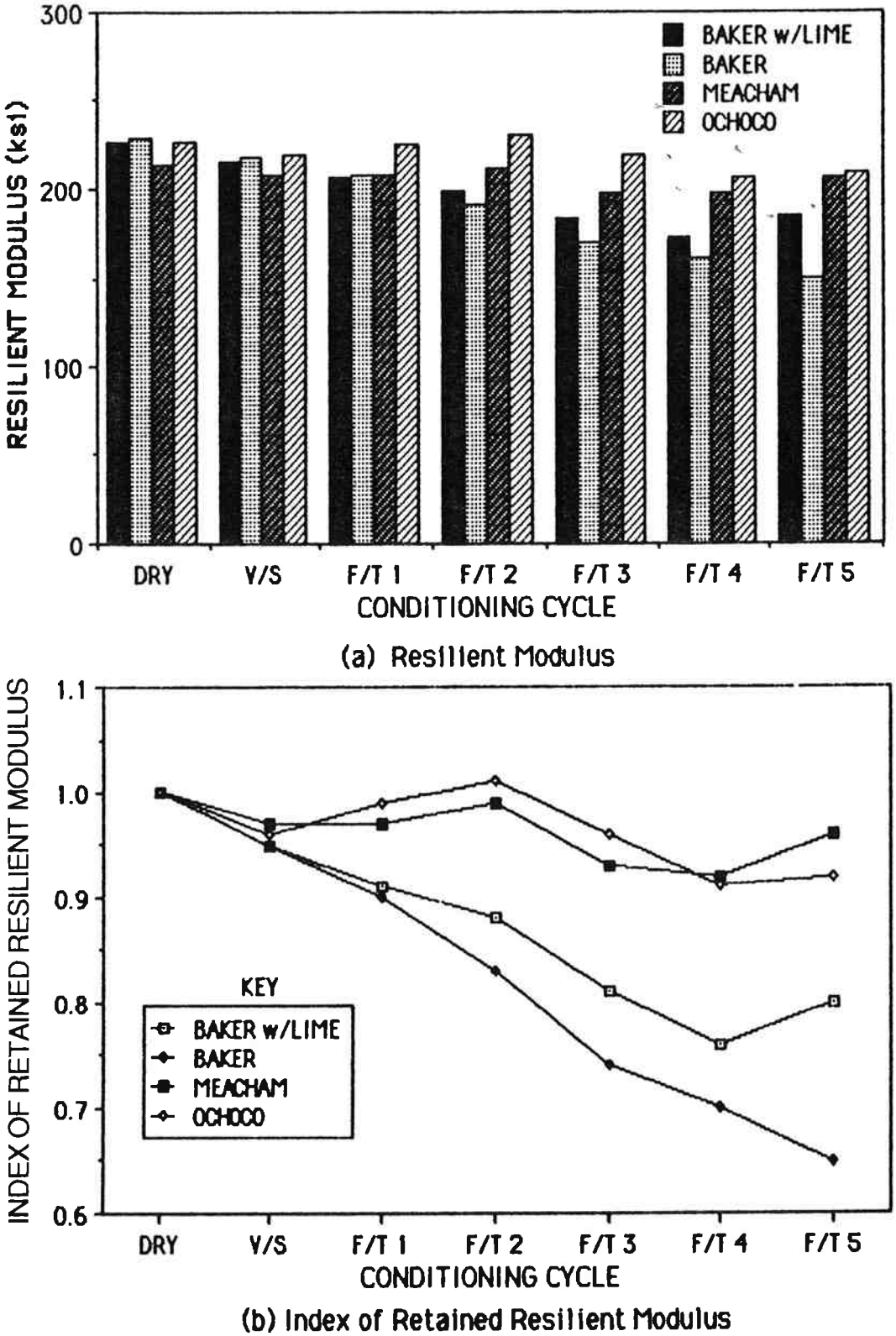

FIGURE 5. Resilient Modulus and Index of Retained Resilient Modulus vs. Conditioning Cycle.

average moduli of both Baker rock mixtures until the first freeze/thaw cycle, and they are never higher than the average moduli of the Ochoco rock mixtures.

5) The moduli of each group recover at the second freeze/thaw cycle. This phenomenon is least noticeable for the untreated Baker rock mixture, and very pronounced for the Meacham and Ochoco mixtures. A similar trend was observed by Kelly, et.al. (1986). Furber (1987) suggests that the aging of the asphalt mixture may increase for non-stripping aggregate during the conditioning process. Thus, the IRM_r of non-stripping mixtures increases until the mixture has been exposed to sufficient conditioning to break the adhesive bond.

The IRM_r of every mixture passes the failure criterion of 0.70 after one freeze/thaw cycle. This is contrary to the results obtained by ODOT Materials Division, which indicated that the Baker rock mixture required lime treatment. Overall, the IRM_r values reported by ODOT are considerably lower than the values obtained in this investigation. Further, the values of resilient modulus from tests performed at ODOT are approximately 30% higher than those obtained at the Oregon State University laboratory. At present, there is no explanation for this discrepency. This suggests the need to thoroughly investigate and compare the procedures used to obtain the resilient modulus and the IRM_r at both laboratories.

As noted in Table 3, the Ochoco specimens have a lower average air voids content and a higher asphalt cement content than the other mixtures

employed in this study. It is well known that the air voids content has a pronounced effect on the tensile strength and modulus of moisture conditioned asphalt concrete mixtures (Schmidt and Graf, 1972; Hicks et.al., 1985; Kelly et.al., 1986; Dukatz and Phillips, 1987). By reducing the available void space, less moisture can enter the specimen and create damage. Therefore, the modulus remains higher. Also, Schmidt and Graf (1972) concluded that increasing the percentage of asphalt cement substantially increases the IRM_r. Therefore, the increase from 6.2% to 6.5% asphalt content further increases the moisture resistance of the Ochoco rock mixture. Although these effects have not been quantified in this investigation, the evidence strongly suggests that the IRM_r values of the Ochoco mixture would have been lower if the air voids and asphalt cement content had been equal to those of the other mixtures.

The effects of aging are presented in Figure 6. These data indicate that the moduli of the unconditioned specimens increased from 10 to 20% over the 12 day testing period. The effect of aging may be included in the previously determined IRM_r values by increasing, and in two cases decreasing, the original dry modulus (denominator of the IRM_r) of each specimen by the percentage shown in Figure 6. The IRM_r values that result from applying this correction are shown in Figure 7.

The following comparisons between Figures 6 and 7 may be noted:

1) The IRM_r values of the Meacham and Ochoco mixtures are differentiated in Figure 7. The performance of the Meacham mixture is better than the Ochoco mixture after the first freeze/thaw cycle.

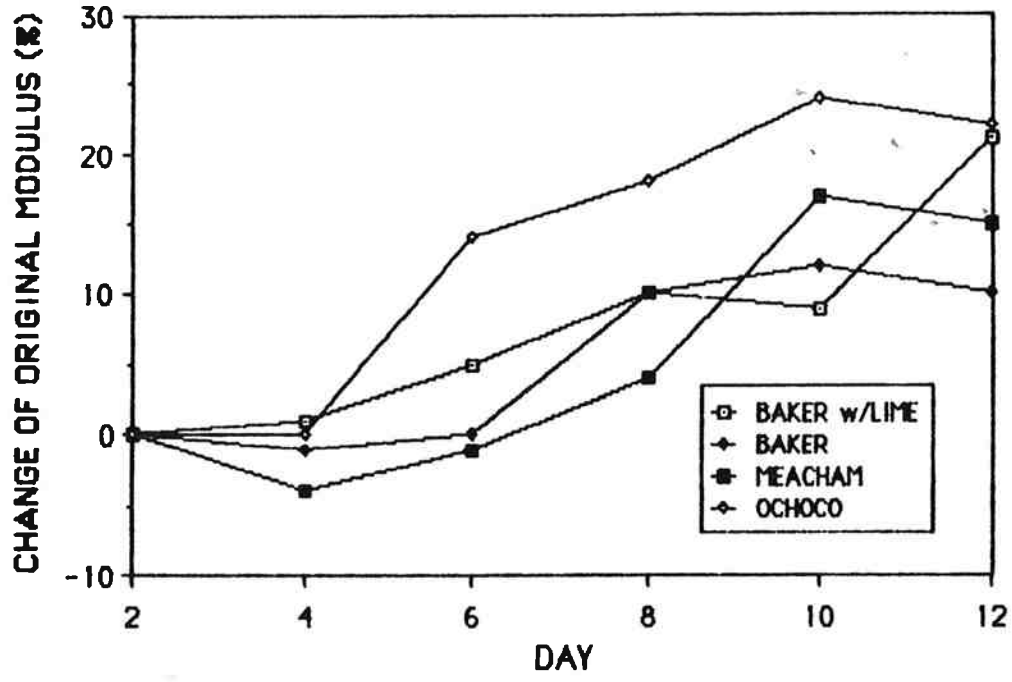

FIGURE 6. Effects of Asphalt Aging on Control Specimens.

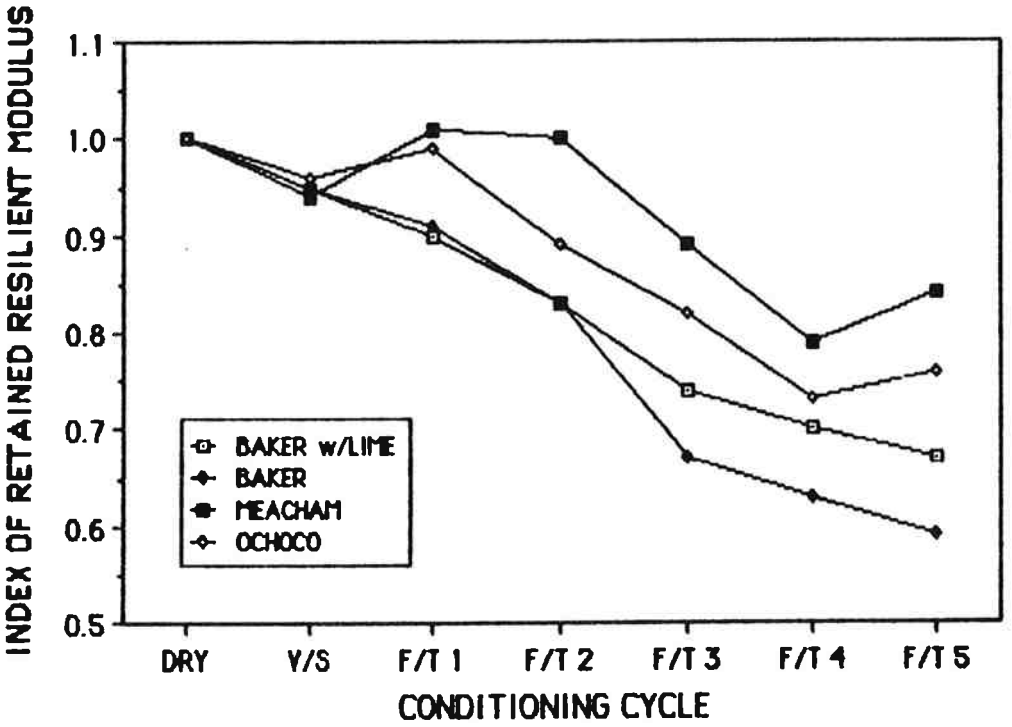

FIGURE 7. Corrected Index of Retained Resilient Modulus vs. Conditioning Cycle.

2) The improved performance of the lime-treated Baker aggregate is less pronounced and does not appear until after the third freeze/thaw cycle.
3) Although the IRM_r values are lower, each mixture would pass the failure criterion of 0.70 after one freeze/thaw cycle.

Fatigue Life Tests

As discussed in Section 3, fatigue life results may be presented in terms of load repetitions to failure as a function of initial tensile strain or tensile stress. Figure 8 shows the relationship between fatigue life and initial tensile strain. This data represents three tests on each group of conditioned specimens. Similarly, Figure 9 shows the relationship between fatigue life and tensile stress. The regression constants for both relationships are given in Table 4.

A comparison of the fatigue lives of each group as a function of initial tensile strain is shown in Figure10. These curves indicate that the lime-treated Baker rock mixture has the longest fatigue life, followed by Ochoco, Baker (untreated), and Meacham, respectively. However, this interpretation ignores the magnitude of load that each specimen experiences.

Tensile strain is a function of both the load magnitude and the modulus of the material. For any given load, a high modulus material has smaller tensile strains than a low modulus material. Therefore, to compare mixtures with different moduli at the same initial tensile strain requires that the load magnitude be decreased for the lower modulus material. This suggests that the relationship between fatigue life and tensile stress may better indicate the reduction of fatigue life associated

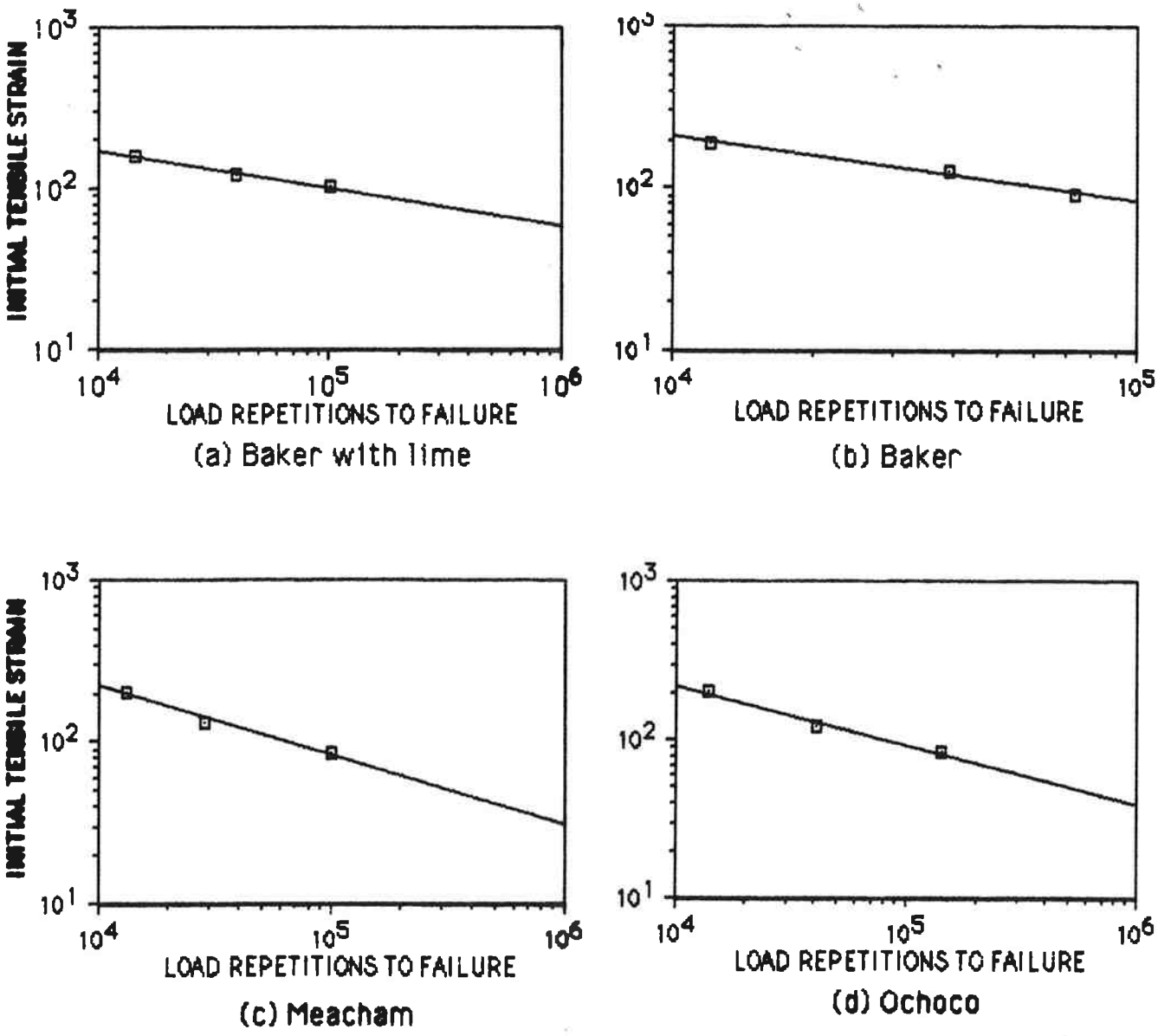

FIGURE 8. Fatigue Life vs. Initial Tensile Strain.

TABLE 4. Regression Constants for Fatigue life Test Relationships.

AGGREGATE SOURCE	FATIGUE LIFE AS FUNCTION OF INITIAL TENSILE STRAIN			FATIGUE LIFE AS FUNCTION OF TENSILE STRESS		
	C	m	R *	K	n	R *
Baker w/Lime	1490	0.234	0.99	102	0.206	0.99
Baker	8120	0.396	0.99	265	0.324	1.00
Meacham	11600	0.429	0.99	688	0.379	1.00
Ochoco	6760	0.372	0.99	444	0.337	0.99

*R = coefficient of correlation

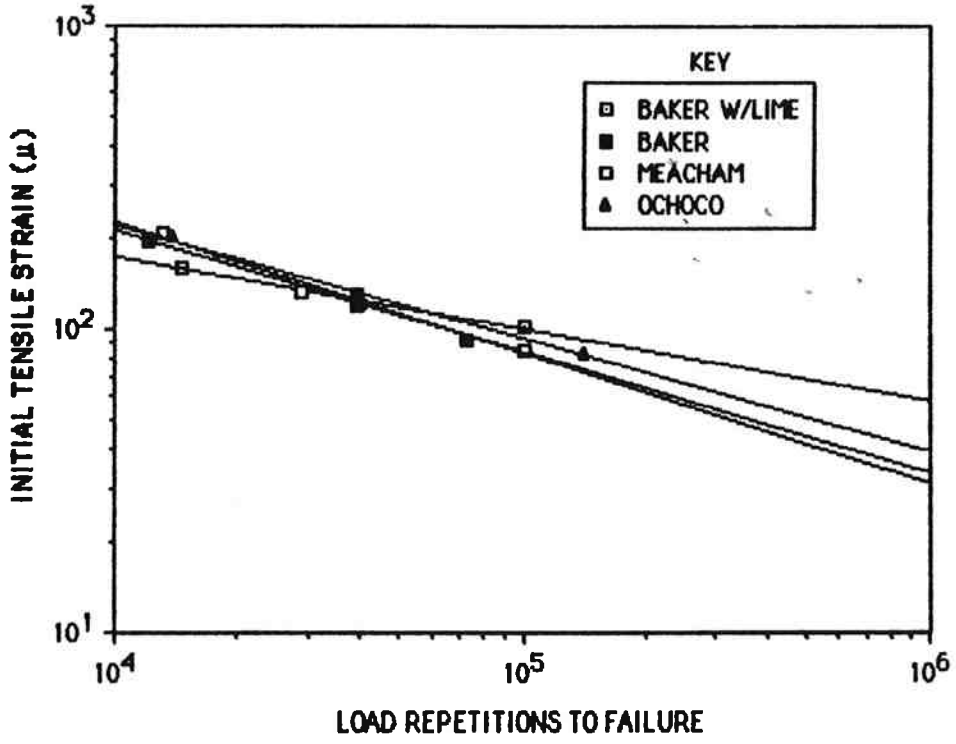

(a) Fatigue Life Vs. Tensile Strain

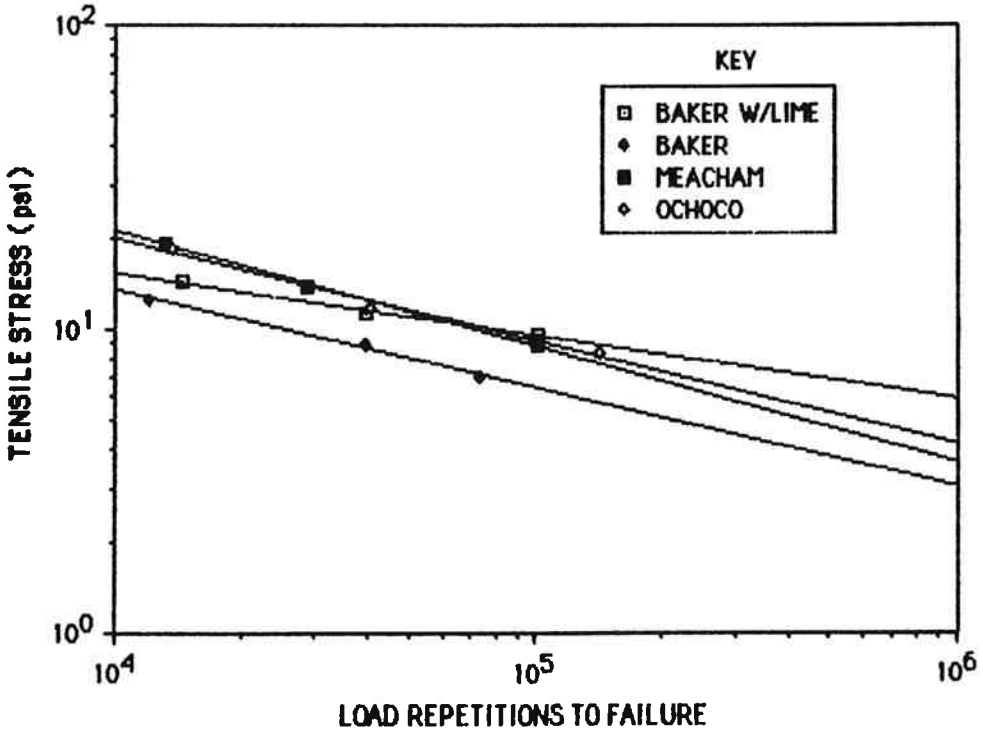

(b) Fatigue Life Vs. Tensile Stress

FIGURE 10. Comparison of Fatigue Life Curves.

with moisture induced distress for mixtures with different moduli.

A comparison of the fatigue lives as a function of tensile stress appears in Figure 10b. The curves shown in Figure 10b clearly indicate that the fatigue life of the Baker rock mixture is significantly lower than the other mixtures. Further, the beneficial effect of lime treatment is evident. There is little difference in the fatigue life of the Ochoco and Meacham mixtures.

The increase of initial tensile strain was measured as a function of fatigue life for each specimen during the performance of the fatigue life tests. This was accomplished by stopping the test, placing the diametral yoke on the specimen, and measuring the horizontal deflections when the load was reapplied. At least two data points were obtained for all but two specimens. However, owing to the uncertainty of the fatigue life, all the measurements could not be obtained at the same percentage of fatigue life. Figure 11 presents the results of these measurements as the percentage increase of initial tensile strain versus the percentage of fatigue listed.

As noted in Figure 11, the tensile strain increased approximately 100 to 200% during the fatigue life tests. Thus, fatigue life test results based on the initial tensile strain do not accurately characterize the behavior of the material, i.e., the tensile strain does not remain constant at the initial level. Minor's Hypothesis may be employed in an attempt to express the fatigue life in terms of an equivalent tensile strain. Minor's Hypothesis, as applied to the results shown in Figure 11, may be stated as follows: the number of cycles required to cause failure at any given tensile strain is equivalent, in terms of effect, to the number of cycles

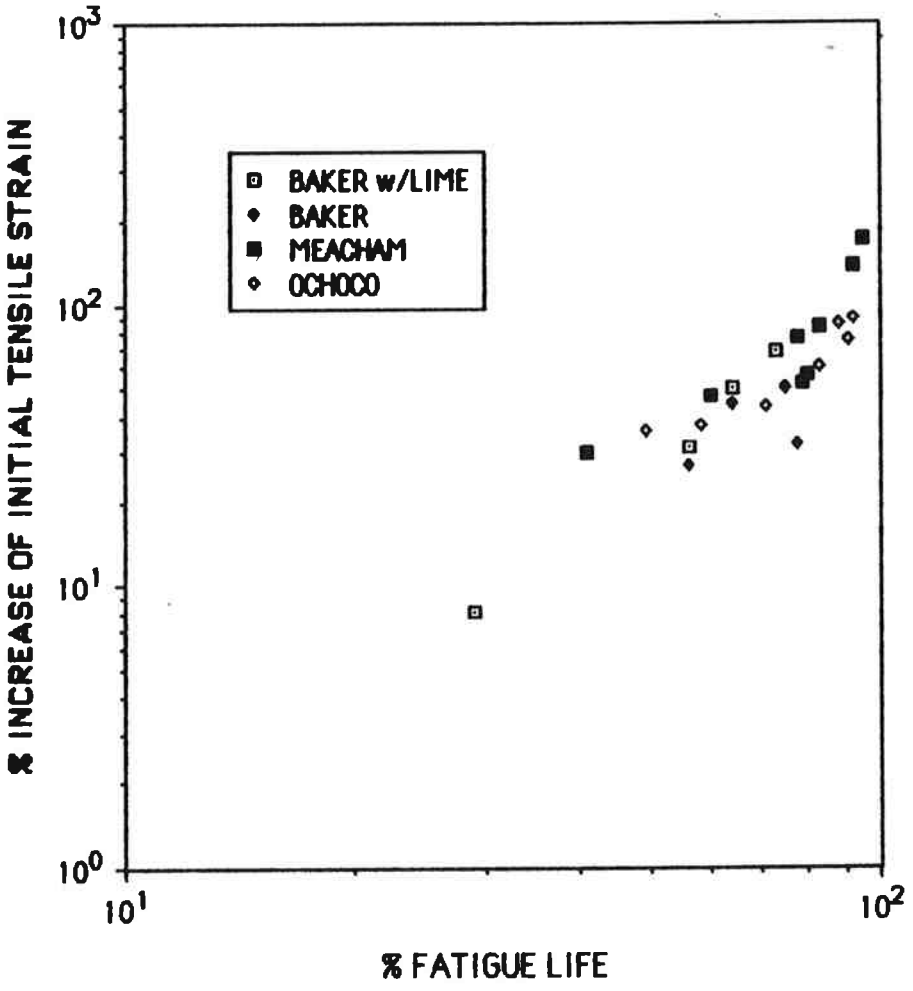

FIGURE 11. Percent Increase of Initial Tensile Strain vs. Percent Fatigue Life.

required to cause failure at any other level of strain. Applying this concept to the average relationship (dashed line) in Figure 11 results in a 20% shift of the fatigue life curves as shown in Figure 12. However, fatigue life relationships obtained in the laboratory are commonly increased by a factor of 10 to 100 times to represent field conditions (Monismith and McLean, 1972). Therefore, the increase represented by Figure 12 may be insignificant from a practical standpoint.

It may further be noted that the relationship shown in Figure 11 could possibly be employed to predict the percentage of fatigue life that a pavement has experienced. Using Equations 3.1 and 3.2, it can be shown that

$$\Delta M_r = 1/\Delta\varepsilon_t \qquad (4.1)$$

where ΔM_r = % change in M_r

$\Delta\varepsilon_t$ = % change in ε_t

The average line relationship of Figure 11 may therefore be used to plot the relationship between ΔM_r and ΔN_f shown in Figure 13.

The significance of Figure 13 may be appreciated by a simple example. Consider a pavement with a known initial value of resilient modulus. Suppose that field cores extracted ten years after construction indicate that the modulus is only 50% of the initial value. Using Figure 13, this would suggest that the pavement has experienced approximately 70% of its service life.

Comparison of Test Results and Aggregate Durability

Based on the results of the resilient modulus tests and fatigue life

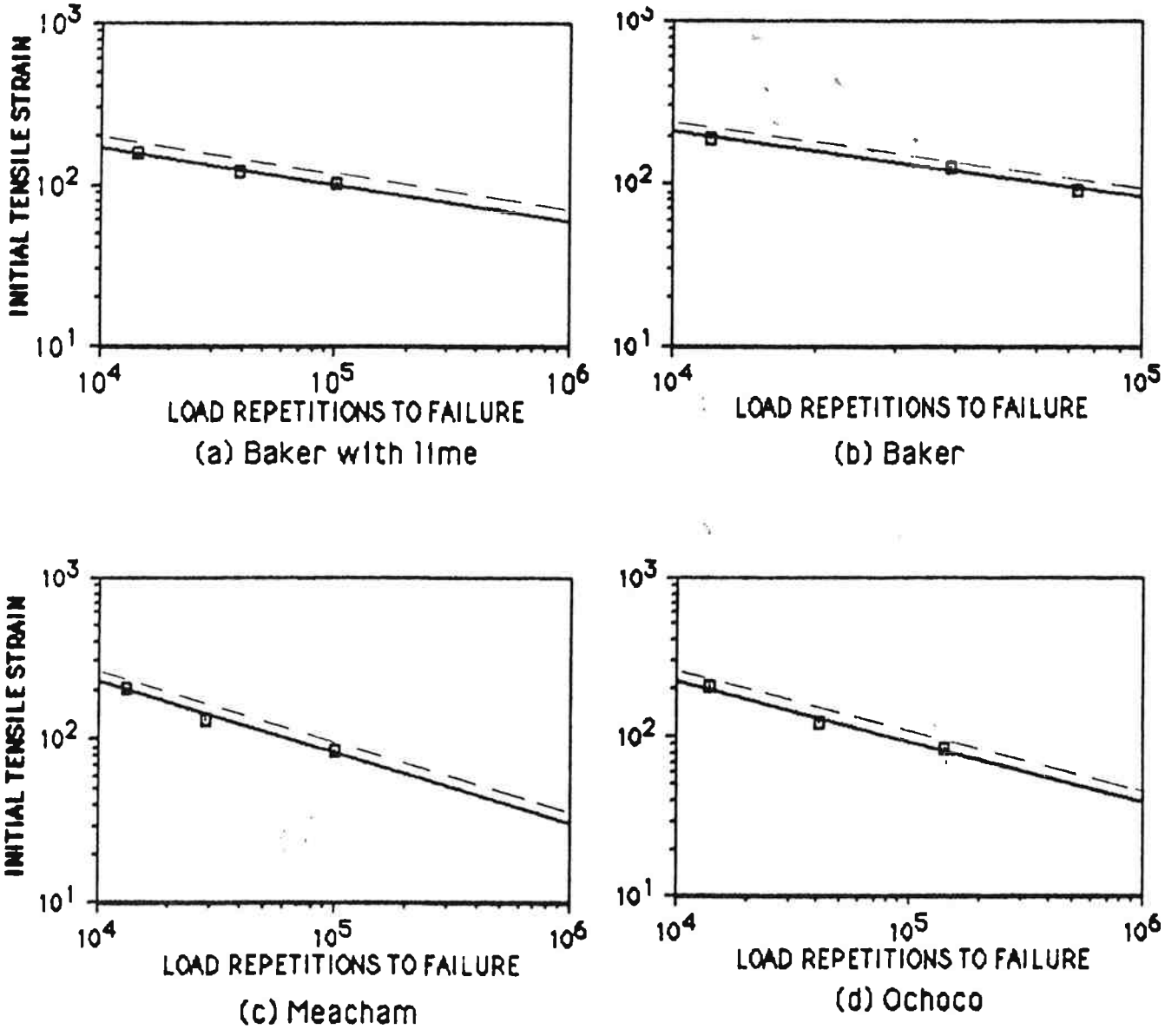

FIGURE 12. Predicted Shift in Fatigue Life Curves Associated with Increase of Initial Tensile Strain.

tests, the moisture-related performance of each group of asphalt concrete mixtures can be rated as follows:

- BakerRock ==>poor to fair
- BakerRock (Lime Treated) ==>fair
- Ochoco ==>good
- Meacham ==>very good

Although the test data appear to rank the Meacham and Ochoco mixtures equally, the variation between the two mixtures (i.e. asphalt cement content and air voids content) clearly provides additional moisture resistance to the Ochoco mixture. Therefore, it can be argued that the Meacham mixture would out perform the Ochoco mixture under equivalent conditions.

Based on the DMSO weight loss (see Table 2), the asphalt concrete mixtures tested in this investigation performed as expected. Szymoniak et.al. (1986) proposed establishing the failure criterion for the DMSO weight loss at 22%. The Meacham rock has an 8.6%/12.6% weight loss and, therefore, should have a relatively high moisture resistance. The Baker rock has a 17.7%/23.9% weight loss. These values lie on each side of the failure threshold, and indicate that Baker rock is moisture susceptible. The Ochoco rock has a 49.3%/44.9% weight loss, which indicates that it is very moisture susceptible. However, the presence of calcite in the plagioclase matrix is believed to cause the DMSO to overreact (Szymoniak, 1986) and, therefore, the results of the DMSO test on this aggregate are invalid. The good perfomance of the Ochoco aggregate in this study confirms this previous conclusion.

The results of the other degradation tests indicate that the Baker rock is generally the poorest aggregate used in this study. The Oregon Aggregate Degradation Test and the Los Angeles Abrasion Test were not performed on the Meacham aggregate, but the results of the Sodium Sulfate Soundness Test confirm that the Meacham rock is the best aggregate.

The results indicate that a qualitative assessment of an aggregate's potential for moisture-induced distress in asphalt concrete may be made based on the DMSO test. However, no correlations can be made from the data gathered in this investigation for several reasons: 1) the DMSO results obtained for the Ochoco aggregate are invalid for reasons noted previously; thus, any correlation would have to be based on only two data points, 2) the mixtures tested had variation other than the type of aggregate used, and 3) the study was conducted using aggregates with unknown field histories; therefore, the IRM_r results cannot be confirmed.

5.0 CONCLUSIONS

This investigation was conducted to establish the applicability of the DMSO test to determine the potential for moisture-induced damage in asphalt concrete mixtures. Resilient modulus tests and fatigue life tests were performed on conditioned specimens composed of aggregate from three sources. The conclusions of this study, based on the results of these tests and a comparison of these tests to previously determined aggregate properties, are :

1) Several freeze/thaw cycles are required to adequately differentiate the moisture susceptibilities of the asphalt concrete mixtures employed in this investigation. Similarly, several cycles are needed to identify the benefit gained from the use of lime treatment.
2) Correcting the IRM_r values for the increase of modulus associated with aging better distinguishes the performance of the untreated mixtures.
3) Fatigue life test results based on tensile stress are better indicators of the damage induced by conditioning compared to results based on the initial tensile strain.
4) It may be possible to use the reduction of modulus during the performance of fatigue life tests at a constant tensile stress as a basis for the prediction of the remaining service life of a pavement.
5) The DMSO test provides an index value that appears to indicate the moisture susceptibility of asphalt concrete mixtures. However, only a qualitative assessment can be made at present.

6) The measured value of the IRM_r is dependent on many variables and is sensitive to slight deviations in these variables. Therefore, test programs that employ the IRM_r must be carefully designed to control all variables not under investigation.

6.0 RECOMMENDATIONS-IMPLEMENTATION

The results from the research program conducted herein indicate the DMSO test may be used to identify the potential for moisture induced distress in asphalt concrete mixtures. It was not possible to identify a correlation between the DMSO test results and other indicators of pavement performance such as the resilient modulus, IRM_r, or fatigue life . Consequently, at present, only a qualitative assessment of an aggregate's expected performance in asphalt concrete may be made based on DMSO test results.

The IRM_r has been proposed for use by previous investigators as an indicator of moisture - induced distress in asphalt concrete mixes. All resilient modulus tests used in the determination of the IRM_r should be performed at the same level of tensile strain. The strain level should be as low as possible so that the material approaches the elastic range of its stress - strain response. However, the strain level must be large enough so that reasonably accurate horizontal deflections can be measured. All resilient modulus tests used in the determination of the IRM_r must be performed at the same test temperature. These recommendations may be immediately implemented.

7.0 REFERENCES

1. Dukatz, E.L., and Phillips, R.S., 1987, "The Effect of Air Voids on the Tensile Strength Ratio," Paper Presented at the Annual Meeting of the Association of Asphalt Paving Technologists, Reno, NE.
2. Frederickson, C., 1987, Personal Communication, Construction Engineer, Oregon Department of Transportation.
3. Fromm, H.J., 1974, "The Mechanisms of Asphalt Stripping from Aggregate Surfaces," Proceedings, Association of Asphalt Paving Technologists, vol. 43, pp: 191-223.
4. Graf, P.E., 1986, "Factors Affecting Moisture Susceptibility of Asphalt Concrete Mixes," paper prepared for presentation at the Annual Meeting of the Association of Asphalt Pavement Technologists, Clearwater, FL.
5. Hicks, R.G., J.E. Wilson, M.D. Rainey, and J.G. Huddleston, 1985, "Identification & Quantification of the Extent of Asphalt Stripping in Flexible Pavements in Oregon - Phase II," Report No. FHWA-OR-85-3, Materials Division, Oregon Department of Transportation, Salem, OR.
6. Ishai, I., and J. Craus, 1977, "Effect of the Filler on Aggregate-Bitumen Adhesion Properties in Bituminous Mixtures," Proceedings, Association of Asphalt Paving Technologists, vol. 46, pp: 228-258.
7. Karius, H., and J.L. Dalton, 1964, "Detachment of Stone from Binder Under Influence of Water in Road Surface Dressings," Journal of Institute of Petroleum, vol. 50, no. 481, pp: 1-14.
8. Kelly, P.B., R.G. Hicks, A.M. Furber, T.S. Vinson, 1986, "Test Method to Determine the Degree of Asphalt Stripping from Aggregates," Contract No. DTRS-57-85-C-00170, Kelly/Strazer Associates, Inc., Portland, OR.
9. Lottman, R.P., 1978, "Predicting Moisture-Induced Damage to Asphaltic Concrete," NCHRP Report 192, Transportation Research Board, Washington,

D.C.

10. Lottman, R.P., 1982, "Predicting Moisture-Induced Damage to Asphaltic Concrete - Field Evaluation," NCHRP Report 246, Transportation Research Board, Washington, D.C.
11. Majidzadeh, K., and Brovold, F.N., 1968, "State of the Art: Effect of Water on Bitumen-Aggregate Mixtures," Highway Research Board Special Report 98, Highway Research Board, Washington, D.C.
12. Monismith, C.I., and D.B. McLean, 1972, "Structural Design Considerations," Proceedings, Association of Asphalt Paving Technologists, Cleveland, OH.
13. Rice, J.M., 1958, "Relationship of Aggregate Characteristics to the Effect of Water on Bituminous Paving Mixtures," STP 240, American Society for Testing and Materials, pp: 17-34.
14. Schmidt, R.J., and P.E. Graf, 1972, "The Effect of Water on the Resilient Modulus of Asphalt-Treated Mixes," Proceedings, Association of Asphalt Paving Technologists, vol. 41, pp: 118-162.
15. Stuart, K.D., 1986, "Evaluation of Procedures Used to Predict Moisture Damage in Asphalt Mixtures (draft copy)," Report No. FHWA/RD-86/075, Office of Engineering and Highway Operations Research and Development, FHWA, McLean, VA.
16. Sullivan, J., J.E. Wilson, T. George, G. Boyle, R. Delaney, D. Dominick, 1986, "Mix Design Procedures and Guidelines for Asphalt Concrete, Cement Treated Base, and Portland Cement Concrete," Materials Division, Oregon Department of Transportation, Salem, OR.
17. Sullivan, J., 1987, Personal Communication, Maintenance Engineer, Oregon Department of Transportation.
18. Szymoniak, T., T.S. Vinson, J.E. Wilson, 1986, "Development of a Standard Accelerated Weathering Test for Aggregates, Dimethyl Sulfoxide - Volume

I," HPR No. 085-5167, Oregon Department of Transportation, Salem, OR

19. Taylor, M.A., and N.P. Khosla, 1983, "Stripping of Asphalt Pavements. State-of-the-Art," Transportation Research Record 911, Transportation Research Board, Washington, D.C., pp: 150-158.
20. Tunnicliff, D.G., and R.E. Root, 1984, "Use of Antistripping Additives in Asphaltic Concrete Mixtures - Laboratory Phase," NCHRP Report 274, Transportation Research Board, Washington, D.C.
21. Tyler, O.R., 1938, "Adhesion of Bituminous Films to Aggregates," Purdue University Bulletin, No. 62, Vol. 22.

APPENDIX A: INFLUENCE OF BOUNDARY CONDITIONS ON THE DETERMINATION OF RESILIENT MODULUS

The Resilient Modulus Test

The resilient modulus test utilizes a nominal 4-inch diameter cylindrical specimen (Marshall specimen) that is subjected to a repeated load along its diametral axis. A typical configuration of test equipment consists of four major components: 1) a load control cabinet, 2) a load frame, 3) a diametral yoke, and 4) a recording system. A schematic diagram of a test specimen with the diametral yoke and loading ram is shown in Figure A.1. The load frame and diametral yoke may be placed inside an environmental cabinet to achieve the ±1.8°F (±1.0°C) temperature control that is identified in the standard test procedure (ASTM D4123).

The material properties of the test specimen (i.e. resilient modulus and Poisson's ratio) may be calculated as follows:

$$M_r = (P/Ht)\ (\upsilon + .27) \qquad (A.1)$$

where M_r= resilient modulus (psi)

P = repeated load (lbs)

H = total recoverable horizontal deflection (inches)

t = specimen thickness (inches)

υ = Poisson's ratio

and

$$\upsilon = \frac{-3.59\ -0.27\ (V/H)}{0.063\ +\ (V/H)} \qquad (A.2)$$

where

V = total recoverable vertical deflection (inches)

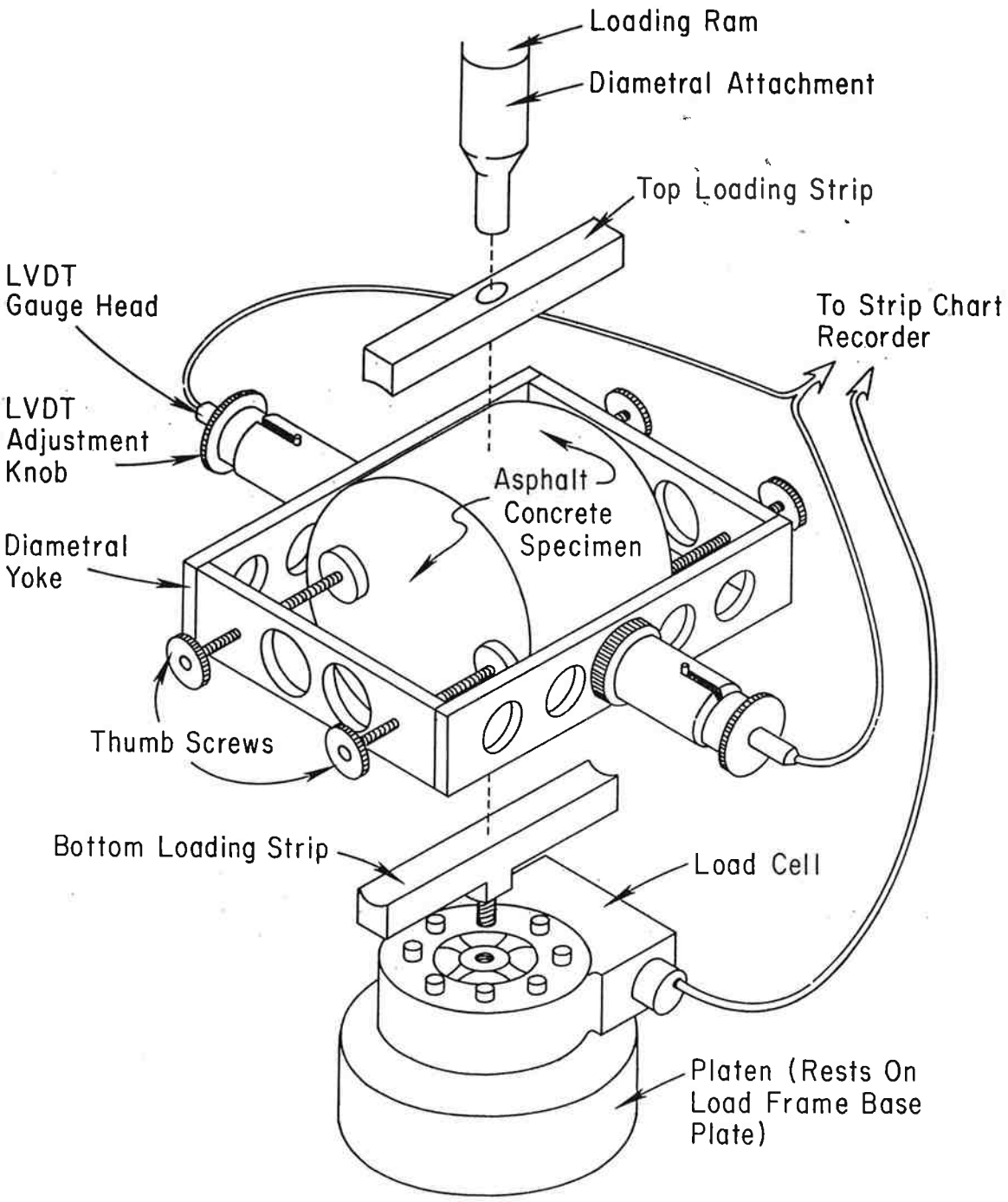

FIGURE A.1. Test Specimen with Diametral Yoke and Loading Ram.

The tensile strain at the center of the specimen is given by

$$\varepsilon_t = \left[\frac{0.16 + 0.48\,\upsilon}{0.27 + \upsilon}\right] H \qquad \text{(A.3)}$$

where ε_t = tensile strain at the center of the specimen (microstrain, μ)

Equations A.1, A.2, and A.3 are supported by the work of Hadley et. al. (1970). He developed equations to evaluate the material properties (i.e. elastic modulus, E, and Poisson's ratio, υ) of diametrically loaded cylindrical specimens. These equations have subsequently been applied to the elastic response of specimens subjected to repeated loads. The following assumptions are made in the development of the equations:

1. The material is elastic, thus Hooke's Law is valid.
2. The material is homogeneous and isotropic, allowing the use of a single value for the modulus and Poisson's ratio.
3. Plane-stress conditions exist and, therefore, the problem can be modeled as two-dimensional.
4. The x- and y- axes are principal planes. This assumption follows from the stress analysis, in which $\tau_{r\theta} = 0$ along these axes.

The stress analysis of a perfectly elastic, homogeneous, isotropic, and weightless, circular element with a diametrically applied compressive strip was performed by Hondros (1959), using a Fourier series. The definition sketch for the theoretical development is shown in Figure A.2. Figure A.3 illustrates the unit stress distributions that result from Hondros' analysis for a 4-inch diameter disk with a 0.5-inch loading

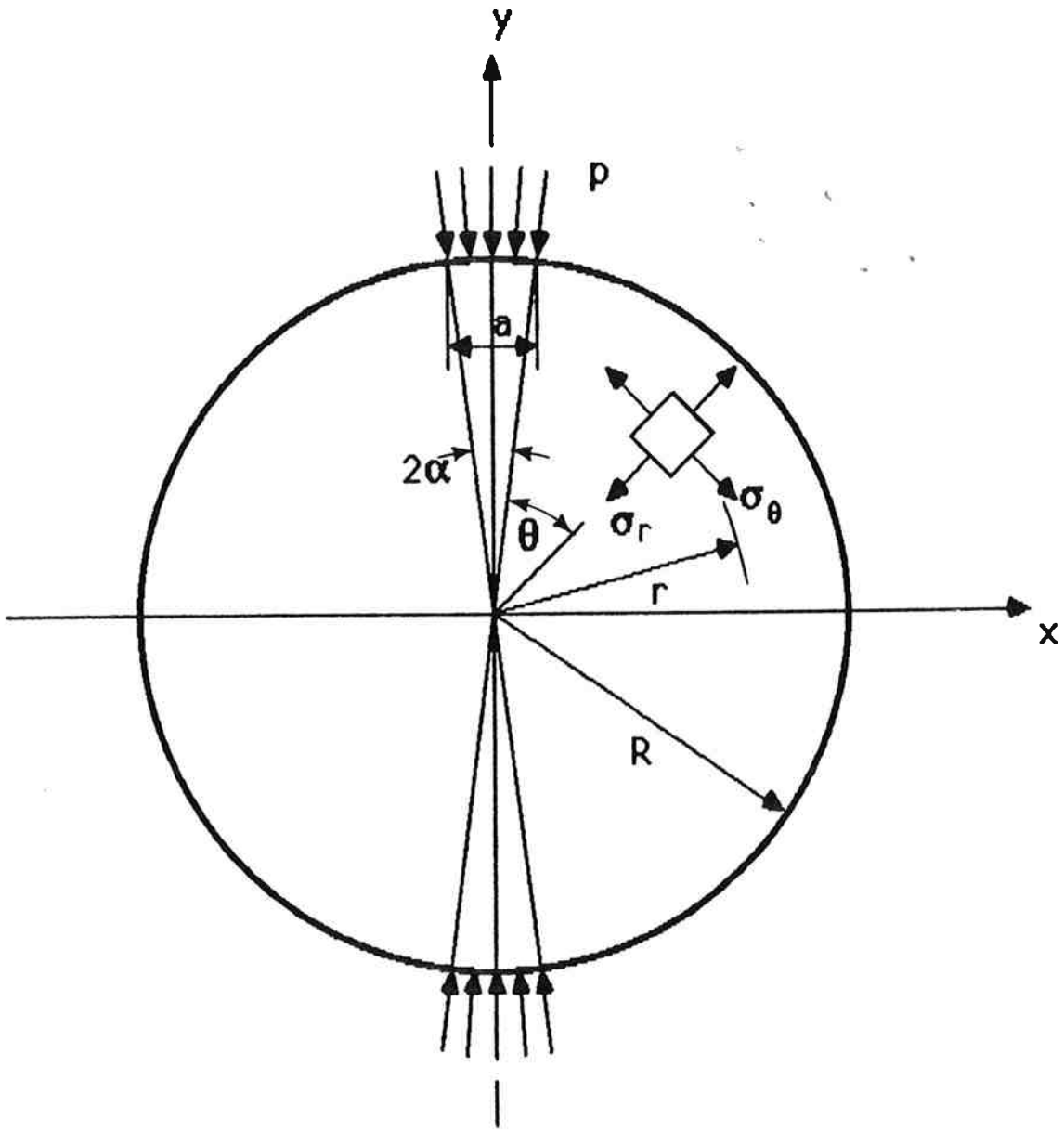

FIGURE A.2. Definition Sketch of a Diametrally Loaded Circular Element.

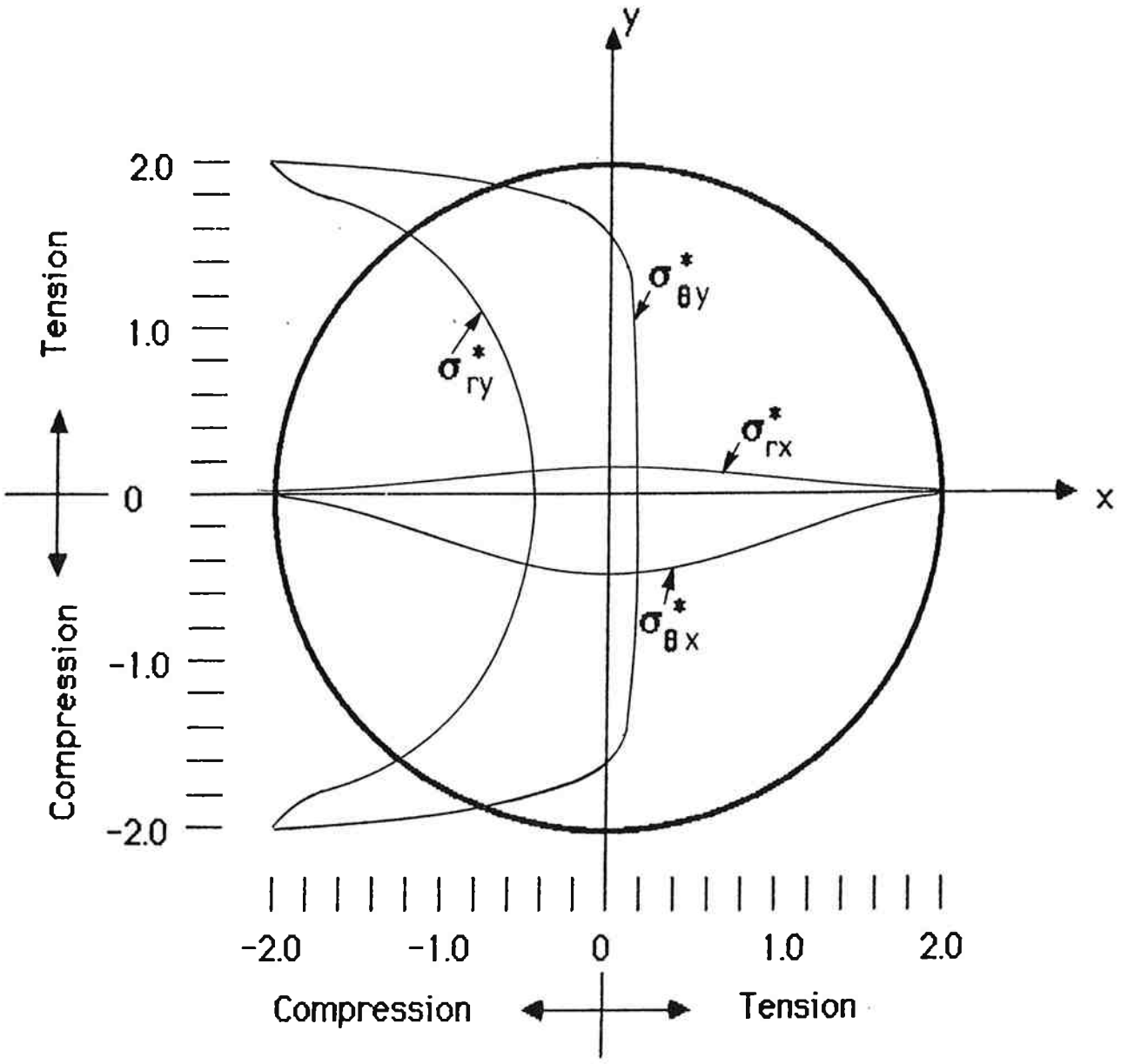

FIGURE A.3. Unit Stress Distribution Along the Vertical and Horizontal Axes for a Diametrally Loaded 4- inch Diameter Circular Element with a 0.5-inch Strip Load (after Hondros, 1959).

strip width.

Any of the four stress distributions ($\sigma_{\theta x}$, σ_{rx}, $\sigma_{\theta y}$, σ_{ry}) can be written

$$\sigma = \pm(2P/\pi at)[f(r,R,\alpha)] \qquad (A.4)$$

If the width of the loading strip is fixed (a = 0.5-inch for this case), Equation A.1 can be rewritten

$$\sigma = (P/t)\left\{2/\pi a\ [\ f(r,R,\alpha)]\right\} = (P/t)\ \sigma^* \qquad (A.5)$$

where σ^*= unit stress

For any differential element along the x-axis, Hooke's Law is expressed as

$$\varepsilon_x = 1/E\ (\sigma_{rx} - \upsilon\ \sigma_{\theta x}) \qquad (A.6)$$

In terms of the total horizontal deflection,

$$H = \int_D \varepsilon_x = \int_D 1/E\ (\sigma_{rx} - \upsilon\ \sigma_{\theta x})$$

from which

$$H = 1/E\ (\int_D \sigma_{rx}\ - \upsilon \int_D \sigma_{\theta x}) \qquad (A.7)$$

where $\int_D$= integral over the diameter

Next, the previously defined expression for unit stress is substituted into Equation A.7 Solving for E,

$$E = P/Ht\ (\int_D \sigma_{rx}^*\ - \upsilon \int_D \sigma_{\theta x}^*) \qquad (A.8)$$

Performing the same operations along the y-axis results in

$$E = P/Vt\ (\int_D \sigma_{ry}^*\ - \upsilon \int_D \sigma_{\theta y}^*) \qquad (A.9)$$

Equations A.8 and A.9 can now be equated to solve for υ,

$$\upsilon = \frac{\int_D \sigma_{ry}^* - \frac{V}{H}\int_D \sigma_{rx}^*}{\int_D \sigma_{\theta y}^* - \frac{V}{H}\int_D \sigma_{\theta x}^*} \qquad (A.10)$$

An equation for tensile strain can now be obtained by first expressingHooke's Law for the deflection over a finite length at the centerof thespecimen,

$$H_l = \int_l \varepsilon_x = \int_l 1/E\ (\sigma_{rx} - \upsilon\ \sigma_{\theta x}) \qquad (A.11)$$

where $\int_l$ = integral over a finite length at the center

By the definition of strain,

$$\varepsilon_{xl} = H_l/l = 1/El\ (\int_l \sigma_{rx} - \upsilon \int_l \sigma_{\theta x}) \qquad (A.12)$$

Expressing Equation A.12 in terms of unit stress and solving for E,

$$E = (P/tl\varepsilon_{xl})\ (\int_l \sigma_{rx}^* - \upsilon \int_l \sigma_{\theta x}^*) \qquad (A.13)$$

The modulus, E, has now been expressed in terms of the total horizontal deflection and in terms of tensile strain . Equating these two expressions results in

$$\varepsilon_{xl} = \frac{H}{l}\left[\frac{\int_l \sigma_{rx}^* - \upsilon \int_l \sigma_{\theta x}^*}{\int_D \sigma_{rx}^* - \upsilon \int_D \sigma_{\theta x}^*}\right] \qquad (A.14)$$

The Mean Value Theorem can now be applied to the expressions $\int_l \sigma_{rx}^*/l$ and $\int_l \sigma_{\theta x}^*/l$ to arrive at

$$\varepsilon_{xl} = H\left[\frac{\sigma_{rx}^*\big|_{r=0} - \upsilon\ \sigma_{\theta x}^*\big|_{r=0}}{\int_D \sigma_{rx}^* - \upsilon \int_D \sigma_{\theta x}^*}\right] \qquad (A.15)$$

where $]_{r=0}$ indicates "evaluated at r = 0"

The expressions for Poisson's ratio, resilient modulus ($M_r = E$), and tensile strain at the center ($\varepsilon_t = \varepsilon_{xl}$) can be solved by numerically

integrating the unit stress over the diameter of the specimen and solving the unit stress at the origin:

$$M_r = (P/Ht)\ (0.27 + \upsilon) \qquad (A.1)$$

$$\upsilon = \frac{-3.59\ -0.27\ (V/H)}{0.063\ +\ (V/H)} \qquad (A.2)$$

$$\varepsilon_t = \left[\frac{0.16 + 0.48\ \upsilon}{0.27 + \upsilon}\right] H \qquad (A.3)$$

It may be noted that the calculation of M_r and ε_t requires the determination of Poisson's ratio. The determination of Poisson's ratio requires measurements of both horizontal and vertical deflections. From a practical standpoint, it is difficult to measure the vertical deflection of a test specimen during the performance of a resilient modulus test. However, if a value of Poisson's ratio is selected as input to Equations A.1 and A.3, the vertical deflection is not needed.

A typical value of Poisson's ratio for asphaltic concrete is 0.35 (Yoder and Witczak, 1975). Based on this assumption, Equations A.1 and A.3 may be rewritten as:

$$M_r = 0.62\ (P/Ht) \qquad (A.16)$$

$$\varepsilon_t = 0.52\ H \times 10^6 \qquad (A.17)$$

The values of M_r and ε_t are obtained using the following procedure:

1) the values of repeated load and horizontal deflection are recorded from tests on two mutually perpendicular diametral axes; and

2) the average value of horizontal deflection (the load usually remains constant) and the value of the repeated load are input to Equations A.16 and A.17.

Finite Element Representation of the Test Conditions

The finite element structural analysis program ANSYS PC/LINEAR (Gorman, 1986) was used to investigate the validity of assumptions 2 (i.e. plane stress condition) and 3 (i.e. loading interface condition) previously noted. The effect of the assumed value of Poisson's ratio on the accuracy of the determination of the resilient modulus was also studied.

Under the assumption of a plane stress condition, the out-of-plane stresses are set equal to zero. However, out-of-plane stresses are present under actual test conditions for the following reasons: 1) the test specimen has a finite thickness which necessarily creates out-of-plane resistance to deflection, and 2) the presence of the thumbscrews, used to attach the diametral yoke (see Figure A.1), provides out-of-plane resistance at their respective locations.

The assumption that a uniform strip load is applied directly to the specimen ignores the surface traction forces and related shear stresses. These forces result from the material incompatibility at the boundary of the steel platen (high modulus) and the test specimen (low modulus). Further, the load distribution is slightly nonuniform owing to the method of application, i.e., a point load is applied to the steel platen at the centerof the test specimen.

The finite element models considered in this study include:

Case 1: plane stress, with a uniformly distributed load applied directly to the circular model;

Case 2: plane stress, with a uniformly distributed load applied to the circular model through a steel loading platen;

Case 3: three-dimensional, with a point load applied to the cylindrical model through a steel loading platen; and

Case 4: three-dimensional, with a point load applied to the cylindrical model through a teflon coated steel loading platen.

The two-dimensional mesh utilized for Case 2 is shown in Figure A.4a. The same mesh is used for Case 1, however the steel loading platen is absent from the model. Only one-quarter of the circular model is needed owing to symmetry. The three-dimensional models can be visualized by expanding the two-dimensional mesh in the z-direction, as shown in Figure A.4b. Again, symmetry may be employed, resulting in a model that represents one-eighth of the test specimen. The actual boundary conditions are simulated in the three-dimensional model by: 1) applying a point load through the steel loading platen to model the loading ram, and 2) restricting the outward (z-direction) deflection of two nodes lying on the x-axis at the position where the thumb screws confine the specimen (see Figure A.4b). No slippage is permitted at the loading interface for Cases 2, 3, and 4.

The resilient modulus test procedure involves first applying a small seating load (5% of the repeated load) to maintain the alignment of the steel platen and the test specimen. The specimen is then subjected to the repeated load. This loading condition (i.e. seating load plus repeated load) could not be modeled using the ANSYS PC/LINEAR program. Therefore the

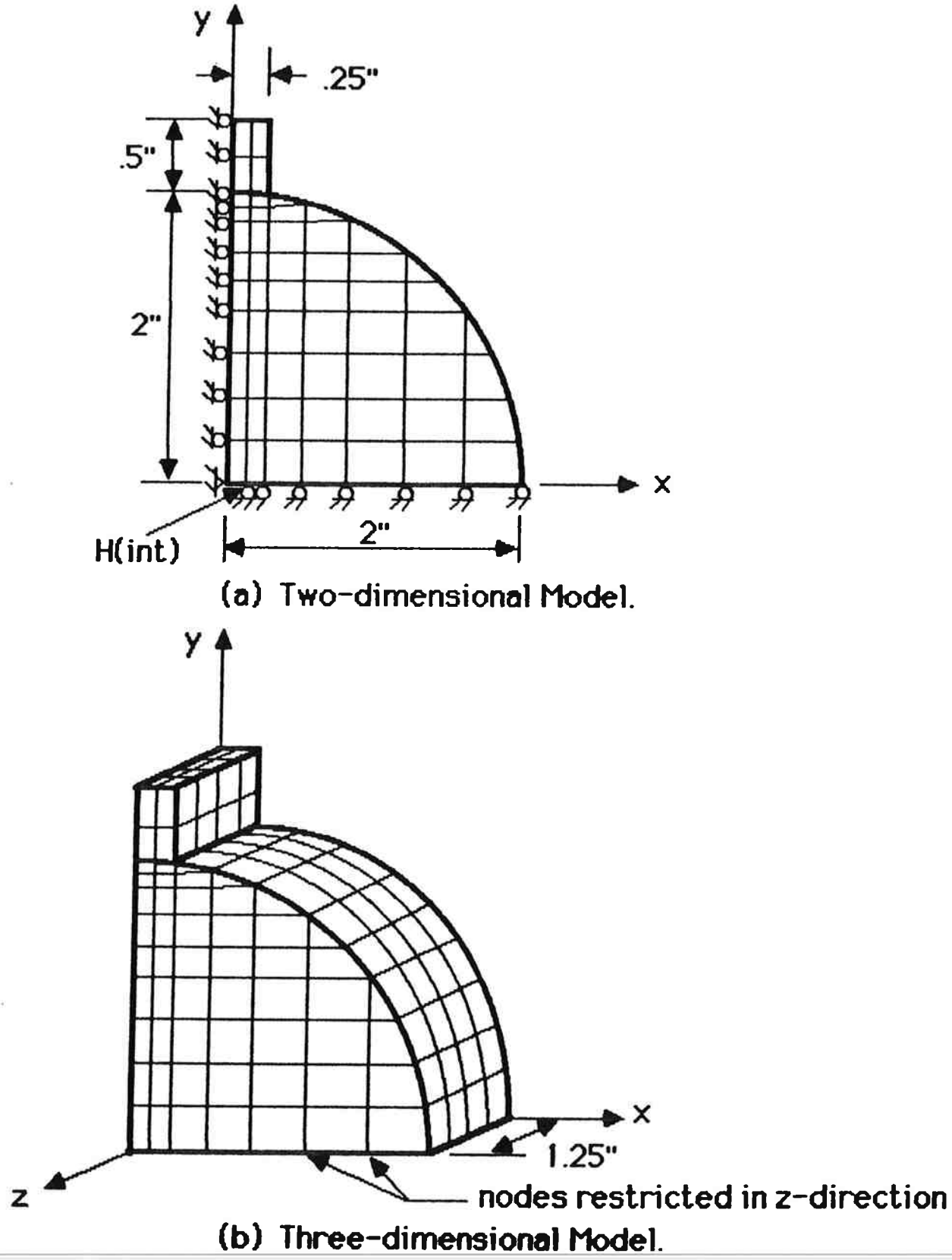

FIGURE A.4. Meshes Utilized in Finite Element Analyses.

initial seating load has been ignored, and a static load was used to represent the repeated load in the analysis. The use of such loading is reasonable, since the model is assumed to be linear elastic.

The following test and material conditions (control conditions) were input to the finite element models:

1) Asphalt concrete properties,

M_r = 300 ksi

υ = 0.35 for Cases 2 and 4

υ = 0.15, 0.35, and 0.45 for Cases 1 and 3

2) Steel loading strip properties,

E = elastic modulus = 29 x 10^3 ksi

υ = 0.30

3) Load (backcalculated using Equations A.1 and A.3 with ε_t = 100μ),

P = 232 lbs

4) Specimen thickness,

t = 2.5 inches

The output from the finite element analyses includes values of horizontal and vertical deflections at each node. These can be used as input to the theoretically developed equations to compare differences between the finite element solution and the theoreticalsolution. Further, the stresses output at each node can be compared to Hondros' theoretical stress distribution.

The deflection results of the finite element analyses, and values backcalculated from these results, are given in Table A.1. The theoretical

solutions, which represent the initial (and compatible) conditions, are identified as control. The resilient modulus is calculated by the following methods:

Method 1. The output values of H and V (total horizontal and vertical deflection obtained from the exterior nodes on the x- and y- axes) are input to Equation A.2 to solve for υ. This computed value of υ, and H and P are used in Equation A.1 to solve for M_r.

Method 2. The control value of υ and P, and the output value of H, are input to Equation A.1 to solve for M_r.

Note that Method 2 represents the typical procedure for the determination of the resilient modulus from laboratory data (i.e. horizontal deflection and repeated load are measured, and υ is assumed). Thus, Method 1 may be viewed as an attempt to improve the estimation of the resilient modulus by obtaining the vertical deflection to calculate the actual value of Poisson's ratio.

The % error and the tensile strain given in Table A.1 are determined as follows:

1) % error equals the difference between M_r(control) and M_r(backcalculated), divided by M_r (control); and
2) tensile strain equals the horizontal deflection of the central element, H(int), divided by the width of the element (0.125 inch).

The Case 1 model best represents the conditions assumed in the theoretical solution. Thus, the accuracy of the mesh employed in this 60

TABLE A.1 Results of Finite Element Analyses

(1) MODEL	INPUT ν	DEFLECTIONS (x .001 inch) (2) H(int)	(3) H	(4) V	METHOD 1 (calculated using vertical and horizontal deflections) (5) ν	(6) Mr (ksi)	(7) % ERROR	METHOD 2 (calculated using horizontal deflections) (8) Mr (ksi)	(9) % ERROR	(10) STRAIN (μ)
CONTROL	0.15	---	0.130	-1.142	0.15	300	0%	300	0%	72
	0.35	---	0.192	-1.182	0.35	300	0%	300	0%	102
	0.45	---	0.223	-1.201	0.45	300	0%	300	0%	117
CASE 1	0.15	0.0088	0.134	-1.102	0.17	304	1%	291	-3%	70
	0.35	0.0125	0.196	-1.098	0.38	306	2%	294	-2%	100
	0.45	0.0143	0.227	-1.096	0.48	307	2%	295	-2%	114
CASE 2	0.35	0.0120	0.195	-0.887	0.53	380	27%	296	-1%	96
CASE 3	0.15	0.0079	0.126	-0.986	0.19	340	13%	310	3%	63
	0.35	0.0110	0.183	-0.985	0.40	341	14%	315	5%	88
	0.45	0.0125	0.212	-0.956	0.53	352	17%	316	5%	100
CASE 4	0.35	0.0111	0.182	-1.099	0.33	305	2%	316	5%	89

study can be verified by comparing Case 1 to the control condition. As noted in Table A.1, the output moduli are within ± 3% for either method of calculation, and Poisson's ratio is within 5%. There is similar close agreement between the tensile strain levels and the stress distributions. Based on this comparison, the accuracy of the finite element representation is acceptable.

The inclusion of the steel platen (Case 2) does not significantly affect the horizontal deflection. Based on Method 2, the output modulus is 1% less than the control modulus and the tensile strain is within 6%. However, owing to the reduction in vertical deflection, Poisson's ratio exceeds 0.50 when Method 1 is employed. This value is theoretically impossible and represents a 50% increase from the control value of 0.35. The resulting value of the resilient modulus is 27% greater than the control value.

The moduli of Cases 3 and 4 that are backcalculated using Method 2 also match the control moduli reasonably well. However, there is a significant difference between the two models when the vertical deflections are considered. Using Method 1, the moduli of Case 3 are from 13 to 17% greater than the control moduli. This represents an error that is approximately 10% greater than the error resulting from Method 2. The Case 4 model behaves in an opposite manner, i.e., the modulus is improved by 3% when the vertical deflections are taken into account. This implies that if measurements of vertical deflection are obtained in the laboratory, the estimate of modulus is not improved unless a low modulus material is positioned between the steel loading platen and the test specimen.

Figure A.5 illustrates Hondros' theoretical unit stress distribution with the nodal unit stress values for Cases 1 through 4 (with $\upsilon = 0.35$) superimposed. The stress values for Cases 3 and 4 represent the weighted average of the nodal stress values along the width (z-direction) of the specimen. The stress distributions along the horizontal axis are practically identical to the theoretical solution for each model, and similar agreement may be noted along the inner two-thirds of the vertical axis. However, the stress distributions diverge at the exterior of the specimen (near the load) as follows: 1) for Case 1, the stresses are almost identical to the theoretical stresses, 2) for Case 4, the vertical stresses decrease by 25% and the horizontal stresses decrease by 50%, and 3) for Cases 2 and 3, the vertical stresses decrease by 50% and the horizontal stresses decrease by 90%.

The differences in stress may be attributed to the effect of surface traction forces that result from the material incompatibility at the loading interface. In the theoretical solution, the horizontal and vertical axes are principal planes (i.e. there are no shear stresses along these axes). However, the finite element models confirm that shear stresses exist along these axes. Thus, the stresses output in the finite element analyses are normal stresses rather than principal stresses. The greater reductions of normal stress for Cases 2 and 3 reflect the high shear stresses that are induced at the load interface. The stresses for the Case 4 model are closer to the theoretical stresses owing to the inclusion of a low modulus material (e.g. teflon, E = 100 ksi) between the high modulus steel and the relatively low modulus asphalt concrete. Comparing Case 4 to Case 3, the shear stresses at the interface are reduced approximately

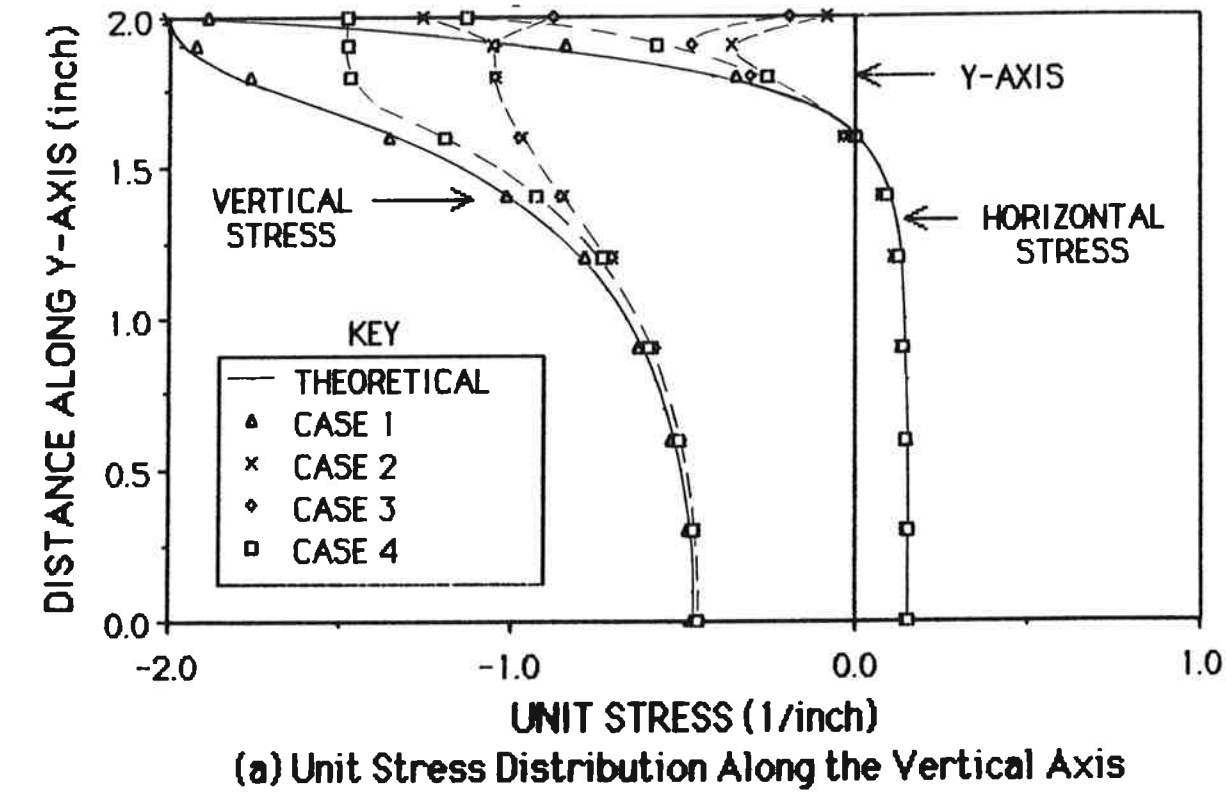

(a) Unit Stress Distribution Along the Vertical Axis

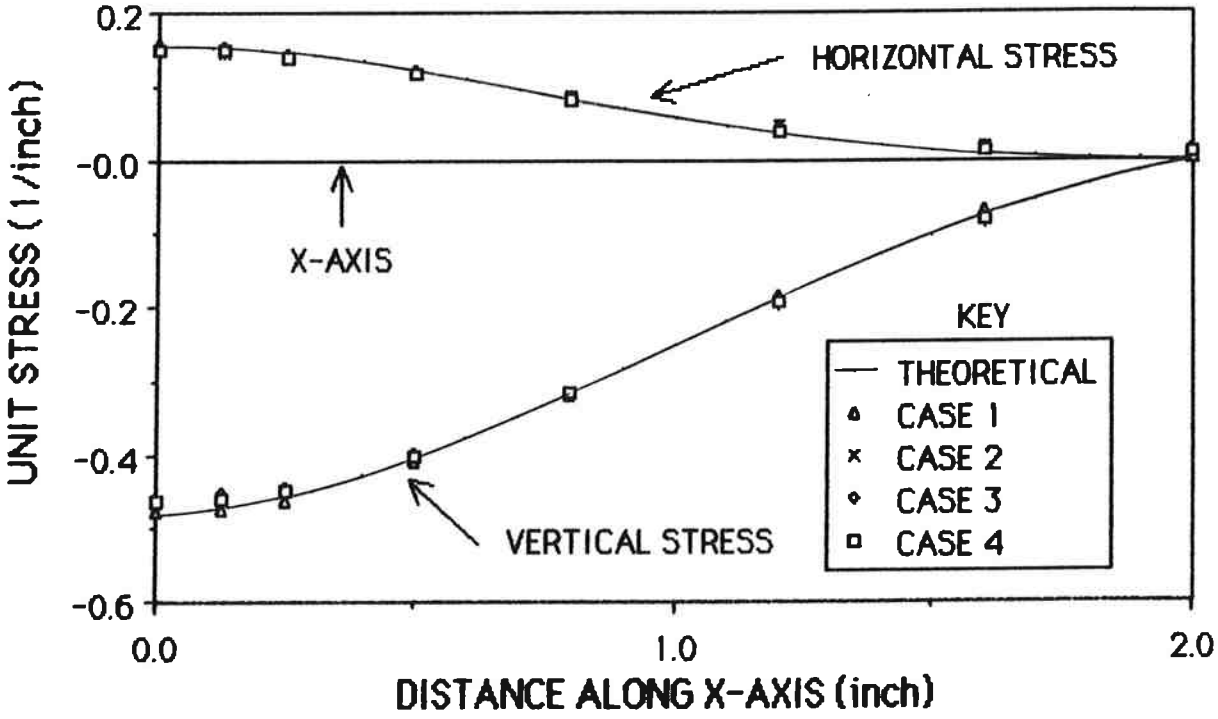

(b) Unit Stress Distribution Along the Horizontal Axis

FIGURE A.5. Comparison of Unit Stress Distributions.

300%.

As previously noted, the stress distributions for Cases 3 and 4 represent the weighted average of stresses across the width of the model. These stresses change from the middle of the model to the free face as follows: 1) the compressive stresses are higher in the middle of the specimen than at the the free face, 2) the tensile stresses are lower in the middle of the specimen than at the free face, 3) the shear stresses are higher in the middle of the specimen than at the free edge, and 4) the out-of-plane compressive stress increases slightly near the location of the thumb screws.

Varying Poisson's ratio from 0.15 to 0.45 has little effect on the accuracy of the estimation of resilient modulus. The backcalculated moduli increase slightly (4% for Case 3) as Poisson's ratio increases from 0.15 to 0.45. Also, the stress distributions are nearly identical for each assumed value of Poisson's ratio.

The results of the finite element models indicate that the resilient modulus diametral test is adequately represented by elastic theory based on the assumption of plane stress response of the test specimen. Although the actual boundary conditions create traction forces that result in the propagation of shear stresses through the specimen, the effect is relatively insignificant with respect to the horizontal deflection actually used in the determination of the resilient modulus. However, if vertical measurements are obtained in an effort to estimate Poisson's ratio, a low modulus material must be placed between the steel load platen and the test specimen.

APPENDIX B: STRAIN AND TEMPERATURE DEPENDENCY OF THE IRM_r

Laboratory Test Program

A laboratory test program was conducted to: 1) develop relationships between the resilient modulus and the tensile strain level and temperature, and 2) establish the significance of these relationships on the determination of the IRM_r. As previously noted, the current test procedure (ASTM D 4123) specifies a temperature tolerance of ±1.8°F (±1°C), and there is no requirement to perform all tests at a specific level of tensile strain.

The asphalt concrete specimens used in the test program were fabricated by the Materials Division of the Oregon Department of Transportation (ODOT). Six 4-inch diameter by 2.5-inch long specimens were prepared using the ODOT Class "C" mix design for heavy traffic (Sullivan et.al., 1986). The specimens were compacted with a Hveem kneading compactor, and air voids contents of approximately 4.6% and 6.8% (three specimens, each) were obtained by varying the the number of blows at the 500 psi level from 150 to 50 blows, respectively. The mix design data and asphalt properties appear in Appendix C.

The test procedure involved the following steps:

1) The bulk specific gravity of each specimen was determined to obtain the air voids contents; the following groups were identified:

   Group 1 ==> 4.6% ±0.4% air voids content

   Group 2 ==> 6.8% ±0.2% air voids content

2) The specimens were allowed to cure for two days.
3) The specimens were placed inside an environmental cabinet

and the temperature was stabilized at the lowest test temperature [36°F (2.1°C)].

4) The resilient modulus test was performed along a randomly selected axis; each test was conducted using a load frequency of 1 Hz and a load duration of 0.1 second; the test temperature was maintained within ±0.2°F (±0.1°C) of the target temperature and monitored using thermistors attached to the sides of the specimens; the load was continually increased, allowing tensile strain and modulus values to be measured at six levels.
5) The specimen was rotated 90° and the procedure was repeated.
6) After testing each specimen, the temperature was increased to the next level and allowed to stabilize overnight.

Steps 3 through 5 were performed using the following temperature levels: 36°F, 53°F, 65°F, 73°F, 81°F, and 92°F (2.1°C, 11.7°C, 18.8°C, 22.8°C, 27.2°C, and 33.1°C). Approximately 300 load repetitions were applied at each level.

Test Results

The results of the test program are plotted in Figure B.1. Figure B.1a presents the log tensile strain vs. log resilient modulus relationship for all tests performed on Group 1. The data for the three specimens are combined corresponding to the six test temperatures. Similarly, Figure B.1b shows this relationship for Group 2.

The regression line equations for each set of data take the general form:

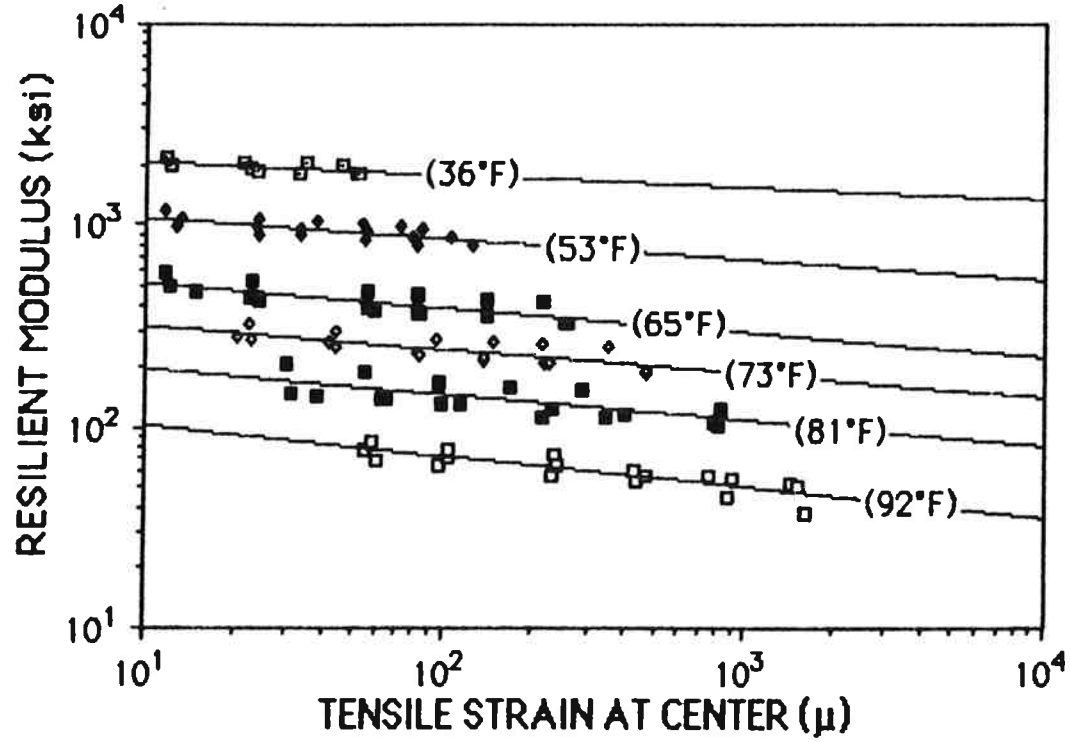

(a) 4.6% Air Voids Content

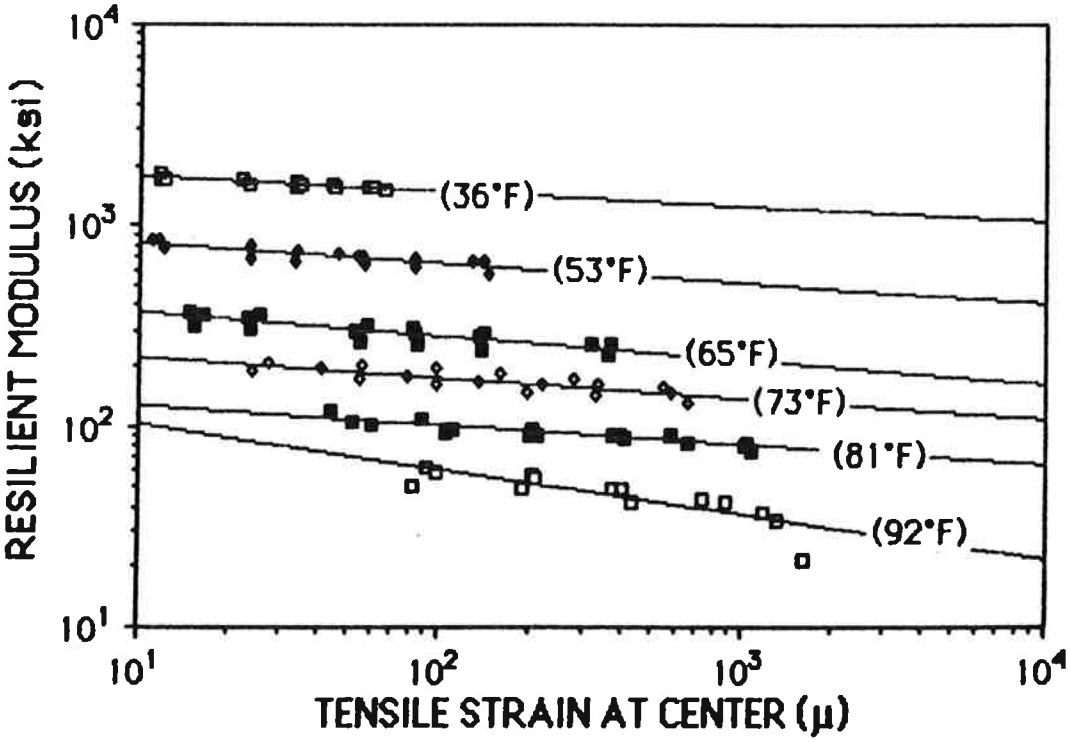

(b) 6.8% Air Voids Content

FIGURE B.1. Resilient Moduli vs. Tensile Strain for the Temperature Range of 36°F to 92°F.

$$M_r = K_1 \varepsilon_t^n \qquad (B.1)$$

where K_1 = a constant evaluated at $\varepsilon_t = 1\mu$ (ksi)

n = a constant representing the slope of the log-log regression line

The values of K_1, n, and R^2 for the regression lines are given in Table B.1

Discussion of Results

As noted previously, the tensile strain vs. resilient modulus data points were obtained at six strain levels. However, fewer data points were obtained at the temperature extremes, namely 36°F and 92°F. At 36°F, the specimens were so stiff that the load limit of the test equipment (i.e., a 1000 lb. load cell) was reached at approximately 50μ to 80μ. At 92°F, permanent deformations were visible at strain levels greater than 1500μ, and one of the Group 2 specimens displayed slight cracking at 1600μ.

The coefficients of determination (R^2 in Table B.1) range from 0.59 to 0.91 for all data. However, if separate regression lines are calculated for each specimen, the R^2 values range from 0.91 to 1.00, with the majority above 0.95. Further, the correlation is better for the specimens of Group 2, which have less variation of air voids contents. Therefore, most of the scatter at each temperature level can be attributed to the variation of the air void contents in each group.

The data display two characteristic trends:

1) The slopes of the regression lines, with minor exceptions, become steeper as the temperature increases. This may simply indicate that the relationship between the tensile strain and the resilient

TABLE B.1. Regression Constants for Log Tensile Strain vs. Log Resilient Modulus Relationships.

(1) GROUP NUMBER	(2) TEMPERATURE (°F)	(3) K (ksi)	(4) n	(5) R^2
1 (4.6% air voids)	36	2369	-0.063	0.59
	53	1384	-0.104	0.73
	65	700	-0.126	0.81
	73	424	-0.122	0.77
	81	258	-0.128	0.75
	92	146	-0.155	0.80
2 (6.8% air voids)	36	2075	-0.074	0.90
	53	1038	-0.103	0.83
	65	475	-0.116	0.87
	73	276	-0.100	0.83
	81	159	-0.099	0.91
	92	125	-0.166	0.89

modulus is likewise dependent upon temperature. However, the strain levels increase with temperature, implying that the strain dependency of the resilient modulus is greater at higher strain levels.

2) The regression lines of Groups 1 and 2 are generally parallel, with Group 2 data displaced downward. Using the regression equations to obtain resilient moduli at the 100μ strain level, the Group 2 moduli are from 71 to 83% less than the Group 1 moduli. Thus, increasing the air voids content by approximately 2% results in a 75% reduction of resilient moduli.

The resilient modulus data can be normalized to illustrate the general trend of the tensile strain vs. resilient modulus. Normalizing the moduli at each temperature level also eliminates the effects of stress history from previously performed tests. The normalized moduli are obtained by dividing the resilient modulus at any given strain and temperature level by the corresponding resilient modulus evaluated at ε_t = 1μ (i.e., the constant K_1). The normalized resilient moduli vs. tensile strain are plotted in Figure B.2. It may be noted that the results shown in Figure B.2 resemble the relationship between normalized dynamic moduli and shear strain shown in Figure 2. Although Figure B.2 represents only one particular asphalt concrete mixture at two air voids contents, a similar relationship may exist for all asphalt concrete mixtures. Such a characteristic relationship would permit the resilient modulus of any asphalt concrete mixture to be estimated at a standard tensile strain by determining the modulus at any other strain level. Figure B.3 shows the

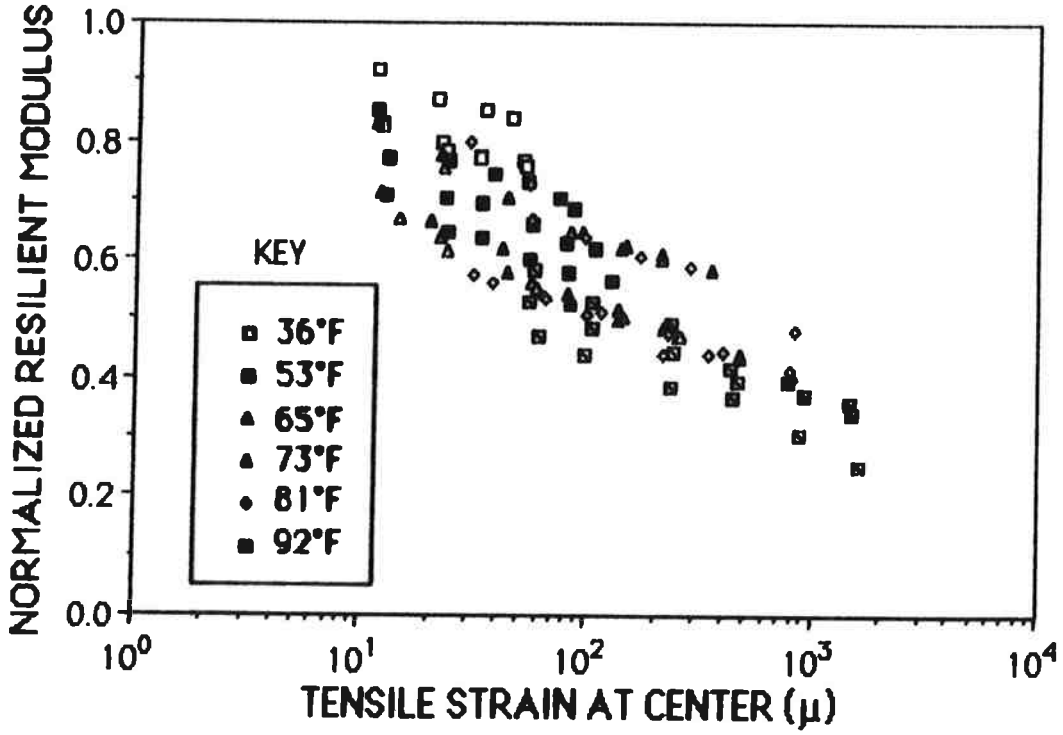

(a) 4.6% Air Voids

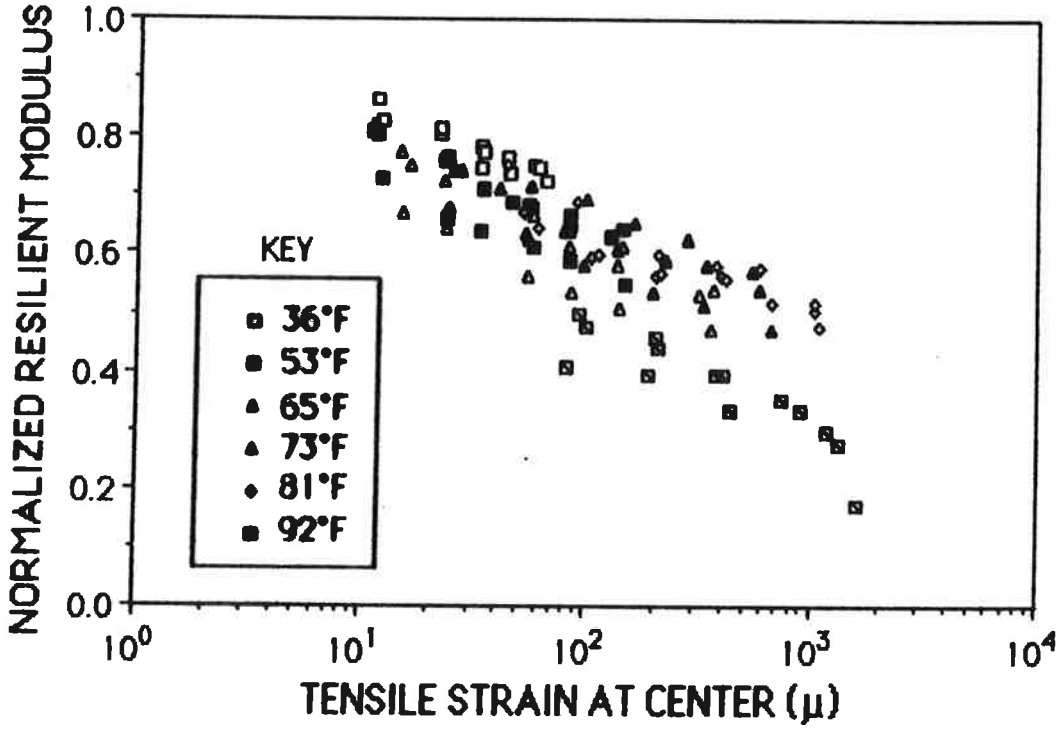

(b) 6.8% Air Voids

FIGURE B.2. Normalized Resilient Moduli vs. Tensile Strain.

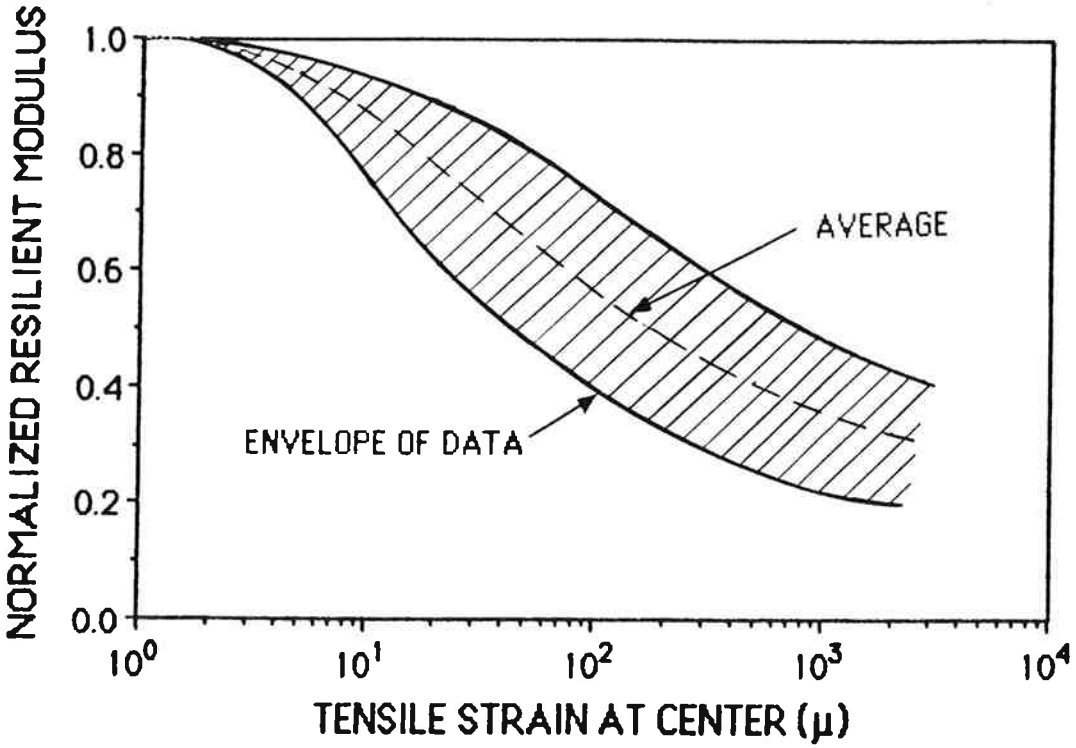

FIGURE B.3. Envelope and Average Relationship for Normalized Resilient Moduli vs. Tensile Strain.

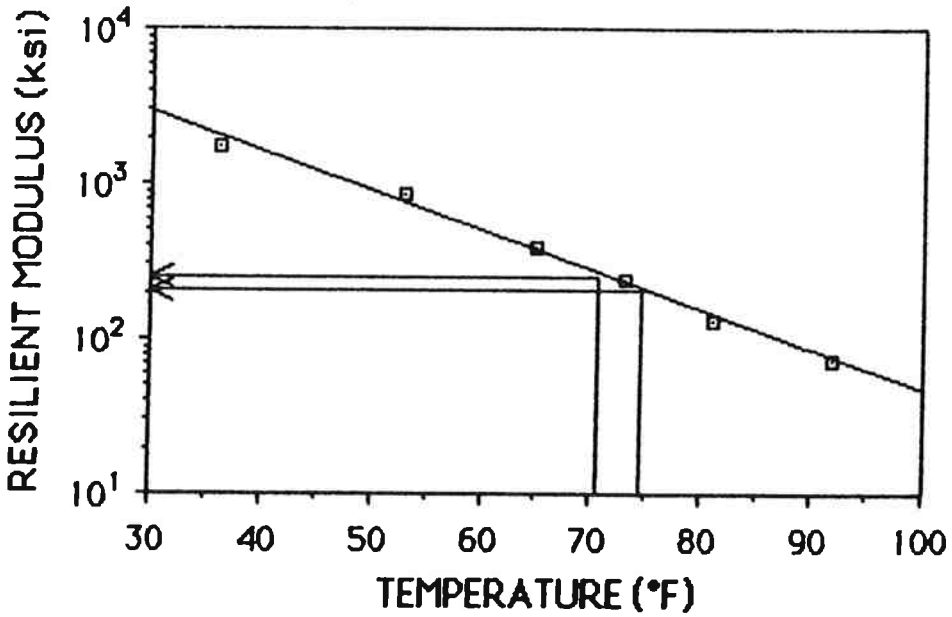

FIGURE B.4. Resilient Modulus vs. Temperature at a Tensile Strain of 100 μ.

envelope and the average relationship between the normalized resilient modulus and the tensile strain for both air void contents.

Figure B.3 can be used to illustrate the significance of the resilient modulus vs. strain relationship on the IRM_r through the following example. Consider two values of resilient moduli such that the resulting IRM_r = 0.70. Let

M_r(control) = 250 ksi, evaluated at $\varepsilon_t = 100\mu$;

M_r(conditioned) = 175 ksi; and

t = 2.5 inches.

Further, consider that the moduli are evaluated under constant load. Then, applying Equation A.17 to the control specimen,

$$H(control) = (100 \times 10^{-6})/0.52 = 0.192 \times 10^{-3} \text{ inch}$$

Substituting H(control) into Equation A.16,

$$P(control) = (250{,}000)(0.192 \times 10^{-3})(2.5)/0.62 = 194 \text{lbs.}$$

P(control) represents the load that would also be used for the test on the conditioned specimen. The value of horizontal deflection for the conditioned specimen may be obtained from Equation A.16,

$$H(conditioned) = (0.62)(194)/(175{,}000)(2.5) = 0.275 \times 10^{-3} \text{ inch}$$

The corresponding strain level may be computed from Equation A.17,

$$\varepsilon_t(conditioned) = (0.52)(0.275 \times 10^{-3}) = 143\mu$$

Entering Figure B.3 at the two tensile strain levels identified above, the appropriate normalized resilient modulus ratios (use average value represented by the dashed line) may be obtained,

for ε_t (control) = 100μ ==> 0..57

for ε_t (conditioned) = 143μ ==> 0..52

The resulting IRM_r is thus determined as,

$$IRM_r = (175/250)\ (0.57/0.52) = 0.77 \quad (\neq 0.70\ !)$$

Note that this does not represent the worst case. For the nominal value of IRM_r = 0.70 determined with the control specimen at ε_t = 50μ and the conditioned specimen at 150μ, the actual value of IRM_r = (0.70)(0.65/0.50) = 0.91. Clearly, the failure to perform both resilient modulus tests at the same tensile strain level results in the misinterpretation of the resulting IRM_r.

The significance of the resilient modulus vs. temperature relationship on the IRM_r can be demonstrated by plotting the resilient modulus vs. temperature at a specific value of tensile strain. Such a plot for ε_t = 100μ is shown in Figure B.4. The allowable temperature extremes for the commonly used test temperature of 73°F (22.8°C) are represented by two vertical lines. Using the regression line as a turning point, the corresponding values of the resilient moduli are 206 and 256 ksi. Obviously, the ratio of any two equivalent moduli must be identically one. However, the ratios of these values (206/256 = 0.81 and 256/206=1.24) identify a range of ±20%. Thus, the failure to conduct each modulus test at the same temperature (but within the test specifications) may result in a ±20% error in the resulting IRM_r.

APPENDIX C: ASPHALT PROPERTIES AND MIX DESIGN DATA

This appendix contains the asphalt properties and the mix design data for the asphalt concrete specimens utilized in the investigation described in Appendix B.

ASPHALT LABORATORY RECORD

Highway Department for Chevron AC-20

Project: Lab Stock
Laboratory Number: 86 18563
Data Sheet Number: None
EA Number: 7517
Date Received: 11-4-86
Date Reported: 11-14-86
Laboratory Charges: $214.00
Contractor: The Oregon Department of Transportation
Submitted By: Chevron
Source of Material: Chevron
Sampled or Inspected At: Portland, Oregon
Sampled or Inspected By: Chevron
Date Sampled: 11-3-86
Quantity Represented: 24 Quarts
To Be Used: M.D.

Paving Asphalt

T 44	Solubility in CHCL: CCL2	99.87%
T 49	Penetration at 77F/39.2 Penetration ratio 39.2/77 F	74/17 cm/100 23
T 201	Viscosity, Kinematic 275 F, 135 C	374 C.S.
T 202	Viscosity, Absolute 140 F	1780 P.

Paving Asphalt RTF (c) Residue

T 47	Loss on Heating	0.81%
T 201	Viscosity, Kinematic 275 F	659 C.S.
T 202	Viscosity, Absolute 140 F, 30 cm Hg., Vac.	6149 P.
T 49	Penetration at 77 F % of orig. penetration	39 cm/100 53%
T 51	Ductility at 77 F	75+ cm

Liquid Asphalt

T 48	Flash Point, open cup	590 °F

APPENDIX C: ASPHALT PROPERTIES AND MIX DESIGN DATA

PRELIMINARY BITUMINOUS MIXTURE DESIGN
Highway Division
Materials Section

Laboratory No. 87 2328
Data Sheet No. AB51156,57
Prefix C10323
Amount Charge $511.00
Date Received 1-23-87
Date Reported

Project— Kelso Road - Mt. Hood Highway
Contractor: Prime— Jim Turin
Paving—
Mix Type Class— C a/c
Contract No.— 10323 Fed. Aid No.— RS-A642(2)
Engineer: Region— Allan C. Harwood Resident— Gary Kennen

AGGREGATE GRADATION: Source— Willamette River #3-104-1 Type— Gravel

Aggregate Size	½ - ¼	¼ - 0					Combined Dry Sieve	Agg Grad Extracted
% Comb.	40	60						
1"								
¾	100 100							
½	99 99						100	100
⅜	63 63	100 100					85	85
¼	10.4 10.4	96.9 96.9					62	62
10	0.9 1.8	51.2 52.1					31	32
40	0.7 1.3	20 20.9					12	13
200 (Dry)	0.7	7.6					4.8	5.0
200 (Wet)	1.1	9.5						
No. Ave.	4	4						

TEST DATA: Asphalt Brand/Grade— Chevron AC-20 Additive—

Percent Asphalt (total mix)	4.5	5.0	5.5	6.0	6.5
Asphalt Film	Dry	Suff	Suff	Suff-Thick	Thick
Sp. Gr. @ 1st Comp. (T-246)	2.33	2.35	2.37	2.39	2.41
Percent Voids @ 1st Comp.	7.7	6.4	4.7	3.2	1.8
Stability @ 1st Comp. (T-247)	34	33	31	36	31
Sp. Gr. @ 2nd Comp.	2.42	2.44	2.46	2.47	2.46
Percent Voids @ 2nd Comp.	4.2	2.8	1.1	0	0
Stability @ 2nd Comp.	41	39	35	38	23
Max. Sp. Gr. (T-209)	2.525	2.511	2.488	2.469	2.455
Index Ret. Str. (T-165) Chevron AC-20	91%		88%		94%
Index Ret. Str. (T-165)					
Index Ret. Str. (T-165)					

Job Mix Formula:

Aggregate Gradation		Asphalt Content:	T-209 TM306	Sp Gr @ 100% Comp	Design Voids @ 100% Comp	@ 1st
1"		Wearing course— 5.6	2.484	2.46	0.9	4.4
¾		Base course— 5.6	2.484	2.46	0.9	4.4
½	100	Shoulder course— 5.6	2.484	2.46	0.9	4.4
⅜	85	PMBB—				
¼	62	Asphalt:				
10	32	Brand— Chevron		Mix Placement Temp.— 280°F		
40	13	Grade— AC-20				
200	5.0	Additive—				

Comments: Qualifying:
87-0754-CA-LAR = 12.1%; NA_2SO_4 = 1.4%; Deg. = 16.3%,0.5"; Friable = 0.8%
87-0755-FA- ————; NA_2SO_4 = 4.7%; Deg. = 9.2%,0.7"; Friable = 0.4%
Asphalt Received 3-6-87

Const.
FHWA
Reg. Engr.
Res. Engr.
Dist. Engr.
Region Geo.
Files

Engineer of Materials

734-1687 (11-81)

APPENDIX D: ASPHALT PROPERTIES AND MIX DESIGN DATA

This appendix contains the asphalt properties and the mix design data for the asphalt concrete specimens utilized in the investigation described in Section 3.0-Test Materials and Procedure.

ASPHALT LABORATORY RECORD

Highway Department for Chevron AC-20

Project: Lab Stock
Laboratory Number: 86 18563
Data Sheet Number: None
EA Number: 7517
Date Received: 11-4-86
Date Reported: 11-14-86
Laboratory Charges: $214.00
Contractor: The Oregon Department of Transportation
Submitted By: Chevron
Source of Material: Chevron
Sampled or Inspected At: Portland, Oregon
Sampled or Inspected By: Chevron
Date Sampled: 11-3-86
Quantity Represented: 24 Quarts
To Be Used: M.D.

Paving Asphalt

T 44	Solubility in CHCL: CCL2	99.87%
T 49	Penetration at 77F/39.2 Penetration ratio 39.2/77 F	74/17 cm/100 23
T 201	Viscosity, Kinematic 275 F, 135 C	374 C.S.
T 202	Viscosity, Absolute 140 F	1780 P.

Paving Asphalt RTF (c) Residue

T 47	Loss on Heating	0.81%
T 201	Viscosity, Kinematic 275 F	659 C.S.
T 202	Viscosity, Absolute 140 F, 30 cm Hg., Vac.	6149 P.
T 49	Penetration at 77 F % of orig. penetration	39 cm/100 53%
T 51	Ductility at 77 F	75+ cm

Liquid Asphalt

T 48	Flash Point, open cup	590 °F

APPENDIX D: ASPHALT PROPERTIES AND MIX DESIGN DATA

PRELIMINARY BITUMINOUS MIXTURE DESIGN
Highway Division
Materials Section

Laboratory No. 87 1343
Data Sheet No. None
Prefix C00087-5167
Amount Charge $551.00
Date Received 12-19-86
Date Reported 2-20-87

Project— DMSO Study Part II
Contractor: Prime— -
Paving— -
Mix Type Class— C a/c
Contract No.— - Fed. Aid No.— -
Engineer: Region— - Resident— -

AGGREGATE GRADATION: Source— Baker Quarry #34-80-1 Type— Quarry

Aggregate Size	½ - ¼		¼ - 0						Combined Dry Sieve	Agg. Grad. Extracted
% Comb.	32		68							
1"										
¾	100	100							100	100
½	94	95							98	98
⅜	41	43	100	100					80	80
¼	6.7	8.0	88	88					62	64
10	2.7	5.0	45.7	46.2					32	33
40	1.6	3.0	22.8	24					16	17
200 (Dry)	0.5		6.3						4.5	5.1
200 (Wet)		1.0		8.8						
No. Ave.	-		-							

TEST DATA: Asphalt Brand/Grade— Chevron AC-20 Additive—

Percent Asphalt (total mix)	4.5	5.0	5.5	6.0	6.5
Asphalt Film	Dry	Dry-Suff	Suff	Suff-Thick	Thick
Sp. Gr. @ 1st Comp. (T-246)	2.30	2.32	2.34	2.36	2.38
Percent Voids @ 1st Comp.	9.8	8.4	6.6	5.1	3.6
Stability @ 1st Comp. (T-247)	37	37	35	34	34
Sp. Gr. @ 2nd Comp.	2.39	2.41	2.43	2.45	2.46
Percent Voids @ 2nd Comp.	6.3	4.9	3.0	2.2	0.4
Stability @ 2nd Comp.	45	45	44	45	37
Max. Sp. Gr. (T-209)	2.551	2.553	2.506	2.486	2.470
Index Ret. Str. (T-165) Chevron AC-20	47%		55%		79%
Index Ret. Str. (T-165)					
Index Ret. Str. (T-165)					

Job Mix Formula:

Aggregate Gradation		Asphalt Content:	T-209 TM306	Sp Gr @ 100% Comp	Design Voids @ 100% Comp	@ 1st
1"		Wearing course— 6.2	2.480	2.45	1.5	4.5
¾	100	Base course— 6.2	2.480	2.45	1.5	4.5
½	98	Shoulder course— 6.2	2.480	2.45	1.5	4.5
⅜	80	PMBB—				
¼	62	Asphalt:				
10	33	Brand— Chevron		Mix Placement Temp.— 280°F		
40	17	Grade— AC-20				
200	5.1	Additive—				

Comments:

Const.
FHWA
Reg. Engr.
Res. Engr.
Dist. Engr.
Region Geo.
Files

Engineer of Materials

734-1887 (11-81)

LABORATORY RECORD

PROJECT TO PREDICT MOISTURE DAMAGE TO ASPHALT PAVEMENT

Page 2 of 2

LABORATORY NO.	87 1344
PROJECT	DMSO Study Part II - Baker Rock
DATA SHEET NO.	None
HIGHWAY	
COUNTY	
EXP. ACCT. SUB JOB	C00085-5167
CONTRACTOR	
F.A. PROJECT NO.	
BID ITEM NO.	
PROJECT MANAGER	
AGY.—ORG. UNIT	
DATE RECEIVED	12-19-86
DATE REPORTED	
TEST NO.	
YEAR	
LAB CHANGE	see page one
For Mix Design Lab. No. -	87-1343
SOURCE OF MATERIAL	Baker Rock #34-80-1
Recommended Asphalt Content -	6.2 %
TO BE USED	Class C a/c without lime

Sample No.	6	7	8	
Asphalt Percentage	4.5	5.5	6.5	
Asphalt Film Thickness	Dry	Suff	Thick	
Bulk Specific Gravity	2.31	2.33	2.37	
Unconditioned Resilient				
Modulus (M_R I) x 10^3	330	324	279	
Strain (x 10^{-6} in.)/Load (lbs.)	51.8 / 130.2	52.6 / 129.6	52.0 / 108.4	
Vacuum Saturated Resilient				
Modulus (M_R II) x 10^3	269	271	269	
Strain (x 10^{-6} in.)/Load (lbs.)	52.6 / 107.8	52.3 / 107.9	51.5 / 103.3	
Freeze-Thaw Resilient				
Modulus (M_R III) x 10^3	49	142	217	
Strain (x 10^{-6} in.)/Load (lbs.)	54.4 / 20.6	52.0 / 56.3	53.3 / 86.5	
M_R Ratio 1 (M_R II/M_R I)	0.82	0.84	0.96	
M_R Ratio 2 (M_R III/M_R I)	0.15	0.44	0.77	

Comments

A minimum of 6.3% asphalt is required for freeze-thaw protection

DISTRIBUTION
Files
Project Manager
Contractor
Region Engineer
Region Assurance Specialist
Region Geologist
Materials - Portland
Materials - Eugene
Glenn Boyle

NOTE: Material represented by this sample does, does not comply with specifications.

Engineer of Materials

APPENDIX D: ASPHALT PROPERTIES AND MIX DESIGN DATA

LABORATORY RECORD
PROJECT TO PREDICT MOISTURE DAMAGE TO ASPHALT PAVEMENT

PROJECT: DMSO Study Part II		LABORATORY NO.: 87 1345	
HIGHWAY	COUNTY	DATA SHEET NO.	
CONTRACTOR	F.A. PROJECT NO.	EXP. ACCT. SUB JOB: C00085-5167	BID ITEM NO.
PROJECT MANAGER	AGY.—ORG. UNIT	DATE RECEIVED: 12-19-86	DATE REPORTED
For Mix Design Lab. No. - 87-1343		TEST NO.	VAR / LAB CHARGE: see page one
SOURCE OF MATERIAL: Baker Rock #34-80-1			
Recommended Asphalt Content - 6.2 %	TO BE USED: Class "C" AC with lime		

Sample No.	9	10	11	
Asphalt Percentage	4.5	5.5	6.5	
Asphalt Film Thickness	Dry	Suff	Thick	
Bulk Specific Gravity	2.28	2.35	2.39	
Unconditioned Resilient				
Modulus (M_R I) x 10^3	324	378	338	
Strain (x 10^{-6} in.)/Load (lbs.)	53.3 / 134	51.2 / 147.6	54.1 / 137.4	
Vacuum Saturated Resilient				
Modulus (M_R II) x 10^3	253	342	311	
Strain (x 10^{-6} in.)/Load (lbs.)	50.5 / 99.2	50.5 / 131.2	51.8 / 120.0	
Freeze-Thaw Resilient				
Modulus (M_R III) x 10^3	69	165	279	
Strain (x 10^{-6} in.)/Load (lbs.)	54.4 / 29.0	52.6 / 66.2	51.5 / 108.2	
M_R Ratio 1 (M_R II/M_R I)	0.78	0.90	0.92	
M_R Ratio 2 (M_R III/M_R I)	0.21	0.44	0.82	

Comments

6.2 % minimum asphalt content is required for freeze-thaw protection

DISTRIBUTION
File
Project Manager
Contractor
Region Engineer
Region Assurance Specialist
Region Geologist
Materials - Portland
Materials - Bituminous
Glenn Boyle

NOTE: Material represented by this sample does, does not comply with specifications.

Engineer of Materials

APPENDIX D: ASPHALT PROPERTIES AND MIX DESIGN DATA

PRELIMINARY BITUMINOUS MIXTURE DESIGN
Highway Division
Materials Section

Laboratory No. 87 1348
Data Sheet No. None
Prefix C00087-5167
Amount Charge $551.00
Date Received 12-19-86
Date Reported 2-20-87

Project— DMSO Study Part II
Contractor: Prime— -
Paving— -
Mix Type Class— C a/c
Engineer: Region— - Contract No.— - Fed. Aid No.— -
Resident— -

AGGREGATE GRADATION: Source— Meacham Quarry #30-15-5 Type— Quarry

Aggregate Size	½ - ¼	¼ - 0					Combined Dry Sieve	Agg. Grad. Extracted
% Comb.	32	68						
1"								
¾	100 100						100	100
½	94 95						98	98
⅜	41 43	100 100					80	80
¼	6.7 8	88 88					62	62
10	2.7 5	45.7 46.2					32	33
40	1.6 3	22.8 24					16	16
200 (Dry)	0.5	6.3					4.5	5.2
200 (Wet)	1.0	8.8						
No. Ave.	-	-						

TEST DATA: Asphalt Brand/Grade— Chevron AC-20 86-18563 Additive—

Percent Asphalt (total mix)	4.5	5.0	5.5	6.0	6.5
Asphalt Film	Dry	Dry-Suff	Suff	Suff	Suff-Thick
Sp. Gr. @ 1st Comp. (T-246)	2.30	2.32	2.34	2.36	2.38
Percent Voids @ 1st Comp.	9.9	8.4	6.8	5.2	3.7
Stability @ 1st Comp. (T-247)	25	25	23	21	23
Sp. Gr. @ 2nd Comp.	2.40	2.42	2.44	2.46	2.45
Percent Voids @ 2nd Comp.	6.0	4.4	2.8	1.2	0.9
Stability @ 2nd Comp.	35	34	31	27	19
Max. Sp. Gr. (T-209)	2.553	2.532	2.510	2.490	2.472
Index Ret. Str. (T-165) Chevron AC-20	87%		89%		92%
Index Ret. Str. (T-165)					
Index Ret. Str. (T-165)					

Job Mix Formula:

Aggregate Gradation		Asphalt Content:	T-209 TM306	Sp Gr @ 100% Comp	Design Voids @ 100% Comp	@ 1st
1"		Wearing course— 6.2	2.483	2.46	1.1	4.6
¾	100	Base course— 6.2	2.483	2.46	1.1	4.6
½	98	Shoulder course— 6.2	2.483	2.46	1.1	4.6
⅜	80	PMBB—				
¼	62	Asphalt:				
10	33	Brand— Chevron		Mix Placement Temp.— 280°F		
40	16	Grade— AC-20				
200	5.2	Additive—				

Comments:

Const.
FHWA
Reg. Engr.
Res. Engr.
Dist. Engr.
Region Geo.
Files

Engineer of Materials

734-1887 (11-81)

APPENDIX D: ASPHALT PROPERTIES AND MIX DESIGN DATA

LABORATORY RECORD
PROJECT TO PREDICT MOISTURE DAMAGE TO ASPHALT PAVEMENT

LABORATORY NO.: 87 1349
PROJECT: DMSO Study Part II
DATA SHEET NO.: None
HIGHWAY:
COUNTY:
EXP. ACCT. SUB JOB: C00087-5167
CONTRACTOR:
F.A. PROJECT NO.:
BID ITEM NO.:
PROJECT MANAGER:
AGY.—ORG. UNIT:
DATE RECEIVED: 12-19-86
DATE REPORTED:
TEST NO.:
YAR:
LAB CHARGE: see page one

For Mix Design Lab. No. -
SOURCE OF MATERIAL: Meacham Quarry #30-15-5

Recommended Asphalt Content - 6.2 %
TO BE USED: Class C a/c

Sample No.	11	12	13	
Asphalt Percentage	4.5	5.5	6.5	
Asphalt Film Thickness	Dry	suff	Suff-Thick	
Bulk Specific Gravity	2.30	2.37	2.39	
Unconditioned Resilient				
Modulus (M_R I) x 10^3	136	327	268	
Strain (x 10^{-6} in.)/Load (lbs.)	50.5 / 52.5	50.5 / 122.8	51.0 / 99.9	
Vacuum Saturated Resilient				
Modulus (M_R II) x 10^3	245	278	247	
Strain (x 10^{-6} in.)/Load (lbs.)	51.0 / 95.2	50.7 / 105.4	51.5 / 92.9	
Freeze-Thaw Resilient				
Modulus (M_R III) x 10^3	170	243	247	
Strain (x 10^{-6} in.)/Load (lbs.)	50.7 / 65.7	53.1 / 96.3	53.3 / 96.1	
M_R Ratio 1 (M_R II/M_R I)	1.80	0.85	0.92	
M_R Ratio 2 (M_R III/M_R I)	1.25	0.74	0.92	

Comments

DISTRIBUTION
Files
Project Manager
Contractor
Region Engineer
Region Assurance Specialist
Region Geologist
Materials - Portland
Materials - Eugene
Glenn Boyle

NOTE: Material represented by this sample does, does not comply with specifications.

734-3008 (6-82)

Engineer of Materials

APPENDIX D: ASPHALT PROPERTIES AND MIX DESIGN DATA

PRELIMINARY BITUMINOUS MIXTURE DESIGN
Highway Division
Materials Section

Laboratory No. 87 1346
Data Sheet No. None
Prefix C00087-5167
Amount Charge $551.00
Date Received 12-19-86
Date Reported 2-20-87

Project— DMSO Study Part II
Contractor: Prime— -
Paving— -
Mix Type Class— C a/c
Contract No.— - Fed. Aid No.— -
Engineer: Region— - Resident— -

AGGREGATE GRADATION: Source— MP60 Mid Top #35-14-5 Type— Quarry

Aggregate Size	½ - ¼		¼ - 0						Combined Dry Sieve	Agg. Grad. Extracted
% Comb.	32		68							
1"										
¾	100	100							100	100
½	94	95							98	98
⅜	41	43	100	100					80	80
¼	6.7	8.0	88	88					62	62
10	2.7	5.0	45.7	46.2					32	33
40	1.6	3.0	22.8	24					16	16
200 (Dry)	0.5		6.3						4.5	5.7
200 (Wet)		1.0		8.8						
No. Ave.										

TEST DATA: Asphalt Brand/Grade— Chevron AC-20 86-18563 Additive—

Percent Asphalt (total mix)	4.5	5.0	5.5	6.0	6.5
Asphalt Film	Dry	Dry-Suff	Suff	Suff-Thick	Thick
Sp. Gr. @ 1st Comp. (T-246)	2.18	2.20	2.22	2.24	2.26
Percent Voids @ 1st Comp.	10.5	9.1	7.3	5.6	4.4
Stability @ 1st Comp. (T-247)	32	35	31	29	29
Sp. Gr. @ 2nd Comp.	2.28	2.30	2.32	2.34	2.34
Percent Voids @ 2nd Comp.	6.4	4.9	3.1	1.7	1.0
Stability @ 2nd Comp.	45	45	46	43	30
Max. Sp. Gr. (T-209)	2.436	2.419	2.395	2.380	2.364
Index Ret. Str. (T-165) Chevron AC-20	56%		66%		75%
Index Ret. Str. (T-165)					
Index Ret. Str. (T-165)					

Job Mix Formula:

Aggregate Gradation		Asphalt Content:	T-209 TM306	Sp Gr @ 100% Comp	Design Voids @ 100% Comp	1st
1"		Wearing course— 6.5	2.364	2.34	1.0	4.4
¾	100	Base course— 6.5	2.364	2.34	1.0	4.4
½	98	Shoulder course— 6.5	2.364	2.34	1.0	4.4
⅜	80	PMBB—				
¼	62	Asphalt:				
10	32	Brand— Chevron		Mix Placement Temp —		
40	16	Grade— AC-20				
200	5.7	Additive—				

Comments:

Const.
FHWA
Reg. Engr.
Res. Engr.
Dist. Engr.
Region Geo.
Files

Engineer of Materials

734-1887 (11-81)

LABORATORY RECORD
PROJECT TO PREDICT MOISTURE DAMAGE TO ASPHALT PAVEMENT

Page 2 of 2

PROJECT: DMSO Study Part II - Mid Top		LABORATORY NO.: 87 1347	
HIGHWAY	COUNTY	DATA SHEET NO.: None	
CONTRACTOR	F.A. PROJECT NO.	EXP. ACCT. SUB JOB: C00087-5167	BID ITEM NO.
PROJECT MANAGER	AGY.—ORG. UNIT	DATE RECEIVED: 12-19-86	DATE REPORTED
For Mix Design Lab. No. - 87-1346		TEST NO. / VAR / LAB CHARGE: see page one	
SOURCE OF MATERIAL: Mid Top Quarry #35-14-5			
Recommended Asphalt Content - 6.5 %	TO BE USED: Class C a/c		

Sample No.	14	15	16	
Asphalt Percentage	4.5	5.5	6.5	
Asphalt Film Thickness	Dry	Suff	Thick	
Bulk Specific Gravity	2.20	2.23		
Unconditioned Resilient				
Modulus (M_R I) x 10^3	365	338	354	
Strain (x 10^{-6} in.)/Load (lbs.)	51.2 / 148.4	51.0 / 134.2	52.6 / 141.5	
Vacuum Saturated Resilient				
Modulus (M_R II) x 10^3	354	345	280	
Strain (x 10^{-6} in.)/Load (lbs.)	52.0 / 146	51.0 / 137.2	52.8 / 152.7	
Freeze-Thaw Resilient				
Modulus (M_R III) x 10^3		223	265	
Strain (x 10^{-6} in.)/Load (lbs.)	53.3 / 79.0	51.8 / 89.9	53.6 / 108.2	
M_R Ratio 1 (M_R II/M_R I)	0.97	1.02	1.07	
M_R Ratio 2 (M_R III/M_R I)	0.55	0.66	0.75	

Comments

6.0% minimum asphalt content is required for freeze-thaw protection

DISTRIBUTION
Files
Project Manager
Contractor
Region Engineer
Region Assurance Specialist
Region Geologist
Materials - Portland
Materials - Eugene
Glenn Boyle

NOTE: Material represented by this sample does, does not comply with specifications.

Engineer of Materials

APPENDIX E: RESILIENT MODULUS AND FATIGUE LIFE TEST DATA

This appendix contains the asphalt properties and the mix design data for the asphalt concrete specimens utilized in the investigation described in Section 4.0-Results and Discussion.

TABLE E.1. Resilient Modulus Test Data for Conditioned Specimens.

		RESILIENT MODULUS (ksi)							
SOURCE	CONDITION	#1	#2	#3	#4	#5	AVERAGE	STD. DEV.	IRM
Baker with 1.0% Lime	Dry	243	227	221	217	224	226.5	10.1	1.00
	V/S	231	219	224	195	205	214.8	14.5	0.95
	F/T 1	246	209	211	170	196	206.6	27.5	0.91
	F/T 2	215	199	202	179	197	198.4	12.7	0.88
	F/T 3	189	194	184	163	189	183.8	12.1	0.81
	F/T 4	163	173	163	179	186	172.7	10.0	0.76
	F/T 5	186	192	186	162	196	184.4	13.1	0.81
		#7	#8	#9	#10	#11			
Baker	Dry	221	236	230	219	243	229.6	10.1	1.00
	V/S	211	217	197	222	244	218.1	17.1	0.95
	F/T 1	217	226	199	199	196	207.5	13.0	0.90
	F/T 2	181	207	175	213	182	191.4	17.2	0.83
	F/T 3	163	193	161	154	176	169.5	15.6	0.74
	F/T 4	150	200	146	161	147	160.8	22.8	0.70
	F/T 5	144	173	134	153	142	149.2	15.0	0.65
		#13	#14	#15	#16	#17			
Meacham	Dry	212	209	187	229	230	213.4	17.6	1.00
	V/S	210	214	189	206	222	208.0	12.3	0.97
	F/T 1	221	213	179	215	212	207.9	16.6	0.97
	F/T 2	210	201	180	229	235	210.8	22.2	0.99
	F/T 3	202	195	179	199	215	197.9	12.9	0.93
	F/T 4	192	183	168	210	233	197.2	25.3	0.92
	F/T 5	213	192	180	214	232	205.9	20.3	0.96
		#19	#20	#21	#22	#23			
Ochoco	Dry	226	204	207	223	275	227.1	28.3	1.00
	V/S	205	184	214	218	274	219.1	33.4	0.96
	F/T 1	244	213	217	218	236	225.6	13.4	0.99
	F/T 2	218	200	229	224	278	229.8	28.9	1.01
	F/T 3	216	202	206	197	271	218.6	30.2	0.96
	F/T 4	211	197	184	214	222	205.7	15.5	0.91
	F/T 5	199	196	183	203	267	209.4	33.1	0.92

APPENDIX E: RESILIENT MODULUS AND FATIGUE LIFE TEST DATA

TABLE E.2. Resilient Modulus Test Data for Dry (Control) Specimens.

AGE OF SPECIMEN	#6 (Baker w/Lime)		#12 (Baker)		#18 (Meecham)		#24 (Ochoco)	
	Mr (ksi)	% Change*	Mr (ksi)	% Change*	Mr (ksi)	% Change*	Mr (ksi)	% Change*
2 days	216	0	231	0	211	0	226	0
4 days	217	1	228	-1	203	-4	226	0
6 days	226	5	230	0	209	-1	259	14
8 days	238	10	254	10	220	4	268	18
10 days	236	9	289	12	246	17	282	24
12 days	260	21	253	10	243	15	278	22
Air Voids Content	5.6%		4.7%		4.4%		3.6%	

(*) % Change = [Mr - Mr(2 days)] / Mr(2 days)

APPENDIX E: RESILIENT MODULUS AND FATIGUE LIFE TEST DATA

TABLE E.3. Fatigue Life Test Results

SOURCE/ SPECIMEN	INITIAL TENSILE STRAIN (microstrain)	TENSILE STRESS (psi)	FATIGUE LIFE (repetitions to failure)	PERCENT CHANGE OF INITIAL TENSILE STRAIN	PERCENT OF FATIGUE LIFE
Baker w/Lime					
#6	102	9.7	100009	31%	56%
#2	120	11.2	39343	50%	64%
#1	160	14.4	14550	8%	29%
				68%	73%
Baker					
#10	93	6.9	73093	13%	51%
				32%	78%
#11	129	8.9	39348	27%	56%
				51%	75%
#9	193	12.5	12035	6%	44%
				44%	64%
Meacham					
#17	85	8.8	100479	53%	79%
				172%	95%
#13	134	13.8	26852	30%	41%
				77%	78%
				84%	83%
				138%	92%
#15	206	19.1	13132	47%	60%
				56%	80%
Ochoco					
#20	84	8.4	141735	36%	49%
				90%	92%
#19	123	11.8	40301	37%	58%
				86%	88%
#21	201	18.5	13768	74%	91%
				43%	71%